Thaw settlement susceptibility mapping for roads on permafrost - Towards climate-resilient and cost-efficient infrastructure in the Arctic

Scheer, Johanna; Tomaškovičová, Soňa; Ingeman-Nielsen, Thomas

Published in:
Cold Regions Science and Technology

Link to article, DOI:
10.1016/j.coldregions.2024.104136

Publication date:
2024

Document Version
Publisher's PDF, also known as Version of record

Cold Regions Science and Technology 220 (2024) 104136

Contents lists available at ScienceDirect

Cold Regions Science and Technology

journal homepage: www.elsevier.com/locate/coldregions

Thaw settlement susceptibility mapping for roads on permafrost - Towards climate-resilient and cost-efficient infrastructure in the Arctic

Johanna Scheer [*], Soňa Tomaškovičová, Thomas Ingeman-Nielsen [**]

Department of Environmental & Resource Engineering, Technical University of Denmark. Nordvej, Building 119, 2800 Kongens Lyngby, Denmark

ARTICLE INFO

Keywords:
Permafrost hazards
Thaw settlements
Roads
Risk assessment
Arctic communities

ABSTRACT

Permafrost thaw induces terrain instabilities and hazards that severely threaten the integrity of roads and, by extension, the socioeconomic development of Arctic communities. The research aimed at identifying paved road sections currently susceptible to permafrost thaw settlements and their damages, in Ilulissat, West Greenland. To this end, we developed and implemented a Thaw Settlement Susceptibility Index (TSSI) and a mapping framework relying upon the qualitative assessment of hazard sources, infrastructure vulnerability, and impacts of permafrost-induced failures. Our evaluation was principally based on the combination of geotechnical data (including 1127 digitized borehole logs and a high-resolution inventory of road conditions) with remotely sensed ground surface displacement maps. We found that 39% of the roads assessed in Ilulissat were established on highly hazardous terrains, characterized by the presence of fine-grained frost-susceptible sediments, severe water ponding, and/or snow ploughing accumulations. Respectively, 9 and 3% of the road network were evaluated as vulnerable to thaw settlements and severely impacted. Overall, we showed that 12% of paved roads established on sediments were highly susceptible to permafrost thaw settlements and may consequently require greater resources to be maintained. Our study illustrated the potential of hazard and susceptibility maps, produced at the community scale, to support infrastructure risk management and optimization of local resources. Future work will be dedicated to assessing the susceptibility of existing roads and unbuilt terrains to permafrost thaw settlements under projected climate scenarios.

1. Introduction

As the Arctic is warming faster than the rest of the world (AMAP Climate Change, 2019; Rantanen et al., 2022), communities established on permafrost face multiple challenges and risks (Ramage et al., 2022). Extreme climate events and permafrost thaw notably expose Arctic settlements to more frequent and severe hazards (Allard et al., 2012; Haeberli and Whiteman, 2015). In constructed areas, permafrost degradation is exacerbated by the cumulative effects of climate change, and construction and maintenance practices that are often not adapted to current climatic and permafrost conditions. The integrity and serviceability of the built environment are therefore endangered in the prospect of ongoing changes (Hjort et al., 2018; Ingeman-Nielsen et al., 2018; Hjort et al., 2022).

Linear infrastructures traverse heterogeneous terrains with varying permafrost properties and ground ice content (Ingeman-Nielsen et al., 2018; Doré et al., 2022). For this reason, roads are significantly exposed to landscape disturbances and geohazards and are thereby susceptible to damages and disruptions (Chai et al., 2018; Doré et al., 2022; Hjort et al., 2022). Furthermore, the implementation of engineering mitigation solutions remains logistically and technically unrealistic in consideration of local means, and often exceeds typical construction budgets. As a result, such techniques are rarely applied or limited to critical road sections, and costly maintenance operations are undertaken on a regular basis to ensure the serviceability of transportation routes and drivers' safety (Doré et al., 2022; Hjort et al., 2022). At the circumpolar scale, approximately 130,000 km of roads are currently established on permafrost with high thaw potential hazard by mid-century, under the Representative Concentration Pathway (RCP) 4.5-emission scenario (Hjort et al., 2018). Rehabilitation and replacement costs are expected to increase accordingly (Hjort et al., 2022). Consequently, road embankment designs and construction practices must be adapted to current permafrost conditions while accounting for the effects of engineering activities, environmental and climate changes (Hjort et al., 2022). In this context, assessing permafrost thaw risks to linear infrastructure and

* Corresponding author.
** Corresponding author at: Department of Environmental & Resource Engineering, Technical University of Denmark, 2800 Kgs. Lyngby, Denmark.
E-mail addresses: johanna.scheer@protonmail.com (J. Scheer), thin@dtu.dk (T. Ingeman-Nielsen).

https://doi.org/10.1016/j.coldregions.2024.104136
Received 29 August 2023; Received in revised form 2 December 2023; Accepted 28 January 2024
Available online 2 February 2024

Nomenclature

AHP	Analytical hierarchy process
AL	Active layer
ALT	Active layer thickness
InSAR	Interferometric synthetic aperture radar
GIS	Geographic information system
GTO	Greenland Technical Organization
MAAT	Mean annual air temperature
MAGT	Mean annual ground temperature
PIEVC	Public Infrastructure Engineering Vulnerability Committee
PSHI	Permafrost settlement hazard index
PTP	Permafrost thaw potential
RCP	Representative concentration pathway
TBM	Technical Base Map (by Asiaq Greenland Survey)
TSSI	Thaw settlement susceptibility index
ZAA	Zero annual amplitude

determining their physical and societal conditioning factors (Larsen et al., 2021) is essential to support the cost-efficient and proactive management of road networks at the community scale (Doré and Zubeck, 2009; Hjort et al., 2022). This approach involves mapping permafrost thaw-susceptible areas and quantifying constructions currently affected or at risk of failure. Understanding socioeconomic constraints and local needs is concurrently required to select maintenance and risk reduction strategies adapted to site-specific conditions and availability of local resources.

From an engineering perspective, relatively warm and ice-rich permafrost is particularly hazardous when thawing (Hjort et al., 2022; Li et al., 2022). Rising ground temperatures (Biskaborn et al., 2019) and associated ground ice melting are the sources of thaw subsidence and loss of bearing capacity, which can dramatically impair constructions (Streletskiy et al., 2019; Hjort et al., 2022). Ground surface deformations induced by the active layer (AL) seasonal dynamics and permafrost degradation additionally exert significant stresses on infrastructures (Hjort et al., 2022; Scheer et al., 2023). Thaw settlements, therefore, constitute one of the most widespread threats in permafrost environments (Streletskiy et al., 2019; Ni et al., 2021; Doré et al., 2022; Li et al., 2022). As emphasized by Duvillard et al. (2021), thaw settlement occurrences induced by degrading permafrost have nonetheless been variable, historical data thereby remaining too scarce to document their temporal evolution. Determining the likelihood of thaw settlements under present climate conditions and/or its expected evolution under future climate scenarios is therefore the most suited approach to assess associated hazard levels (Duvillard et al., 2021). Over the last decades, many authors (Nelson et al., 2002; Guo and Wang, 2017; Hjort et al., 2018; Streletskiy et al., 2019; Ni et al., 2021) have dedicated research to characterizing thaw settlement hazards leading to the development of susceptibility indices. Focusing on the significant influence of the ground ice content on climate-induced thaw subsidence, Nelson et al. (2002) first formulated a settlement index as the product of the change in active layer thickness (ALT) - relative to a chosen baseline - multiplied by the volumetric proportion of excess ground ice. The settlement index was implemented at the circumpolar scale under derived climate scenarios using a mathematical solution for the AL thickness and digital maps of ground properties. Other variables contributing to thaw subsidence and hazard occurrences were progressively encompassed in regional assessments, contributing to the diversification of thaw settlement hazard mapping techniques. Traditional geological mapping, aerial-image interpretation and site investigation methods (Allard et al., 2012) are nowadays frequently combined with advanced spatial analysis, remote-sensing and machine learning flows (Hjort et al., 2018; Rudy et al., 2019; Allard et al., 2023), numerical and statistical models (Daanen et al., 2011; Li et al., 2022; Allard et al., 2023; Liu et al., 2023), as well as decision-making approaches (Hong et al., 2014; Hjort et al., 2018). Daanen et al. (2011), for instance, numerically modeled the Permafrost Thaw Potential (PTP) over deglaciated areas of Greenland. The PTP values were then used with the geological substrate's properties and ice content in a decision flow diagram to evaluate hazard levels. Since ecological characteristics such as vegetation, surface water, and snow cover also influence thermal transfers to the ground, Hong et al. (2014) created a Permafrost Settlement Hazard Index (PSHI) integrating such variables. The relative influence of the ground ice content, air temperature, soil texture, snow depth, vegetation, and organic content on permafrost thaw was determined by Analytic Hierarchy Process (AHP) through the attribution of weighted coefficients. More recent studies (Hjort et al., 2018; Ni et al., 2021) have combined some of the previously presented geohazard indices to spatially assess permafrost terrains' susceptibility to thaw settlements.

Nonetheless, these approaches were not elaborated specifically for the case of linear infrastructure, for which not only the distribution of ground ice but also embankment designs and geometry, topography, water and snow accumulations are of concern (Chai et al., 2018; Doré et al., 2022; Scheer et al., 2023b). Due to the coarse resolution of available datasets and models, thaw settlement susceptibility indices, accounting for the effects of these parameters, have rarely been used at the community scale to support risk management and planning. Neglecting the effects of hazardous environmental conditions, which can trigger geohazards even occurring at a greater distance from infrastructure (Doré et al., 2022), may, therefore, result in the occurrence of failures and additional maintenance costs (Hjort et al., 2022). On the other hand, advanced hazard mapping techniques developed in recent studies would often require quantitative data, sometimes remaining unavailable in remote Arctic communities and calling for qualitative or alternative evaluation schemes (Allard et al., 2023).

In order to be useful for planners and policy-makers, hazard maps need to be supplemented by evaluations of the socioeconomic impacts of infrastructure failures induced by permafrost thaw and climate change (Duvillard et al., 2021; Larsen et al., 2021; Doré et al., 2022). In engineering contexts, the risk is mathematically defined as the product between the probability of a hazard to occur within a given time frame and the adverse consequences associated with this event (Faber, 2008; Lavell et al., 2012; Haeberli and Whiteman, 2015). Brooks et al. (2019) exemplified this probabilistic approach by quantitatively evaluating hazards and consequences affecting linear infrastructure on permafrost terrains. Hazards, including thaw settlements, were characterized with reliability analysis methods, and consequences were analyzed based on incurred costs. However, semi-quantitative or qualitative assessments remain better suited when data are lacking and the precise estimation of probabilities and consequences is not feasible. By way of illustration, Allard et al. (2023) developed a semi-quantitative permafrost hazard mapping scheme by combining variables and available datasets that were relevant in Nunavik communities established on permafrost. The authors also demonstrated the potential of qualitative scales and risk matrices to assess various geohazards and their impacts on the communities.

Furthermore, as described in Lavell et al. (2012) and Larsen et al. (2021), risks are both physically and socially constructed, thereby embracing more dimensions than hazard likelihood and consequence severity. Several authors contributed to broadening the engineering-based definition of risks by considering exposure, resilience, vulnerability, adaptive capacity or perceptions as additional determinants of risks in their analysis (Streletskiy et al., 2019; Duvillard et al., 2021; Allard et al., 2023). In their qualitative risk evaluation, Duvillard et al. (2021) made a step forward by encompassing both the terrain susceptibility to permafrost hazards and the sensitivity of alpine infrastructures to hazardous events. The potential level of damage and financial value of existing infrastructures were notably used to characterize their

vulnerability. Finally, the Public Infrastructure Engineering Vulnerability Committee (PIEVC) provided a framework to investigate the vulnerability of infrastructure to climate change (Engineers Canada, 2016; Seto et al., 2012). In addition to the qualitative ranking of hazard likelihood and consequence severity, factors impacting the infrastructure performance, such as maintenance operations, policies, and emergency responses, were considered. Overall, multidisciplinary and holistic approaches allowing for the integration of the i) causes of permafrost thaw-induced hazards, ii) socioeconomic consequences of infrastructure failures, iii) infrastructure vulnerability to disturbances, and iv) communities' adaptive capacity, still need to be developed further.

Building upon previous research, we propose a framework adaptable to different site conditions, datasets, and conceptual definitions of susceptibility and risk. In this paper, we specifically focus on mapping and assessing the susceptibility of roads to permafrost thaw settlement hazards at the community scale. To this aim, we validated our methodology by applying it to the road network of Ilulissat, West-Greenland, using existing geotechnical information, remote sensing data, inventory of infrastructure conditions (Scheer et al., 2023b), and local knowledge. Our study case serves as a proof of concept for the production of decision-support maps adapted to the needs of communities established on thawing permafrost, while providing a methodological basis for the meaningful combination of locally available data.

2. Study area

The settlement of Ilulissat is centrally located on the west coast of Greenland (Fig. 1a) and is the seat of the Avannaata municipality. The mean annual air temperature (MAAT) between 2010 and 2019 was −3.2 °C (data from Cappelen, 2020).

Ilulissat is established in the zone of continuous permafrost (Brown et al., 1998; Obu et al., 2019). During the Holocene deglaciation, fine-grained marine sediments were deposited in the area as a result of marine transgression. The isostatic uplift raised the sedimentary deposits above sea level and exposed them to precipitation and percolation. Permafrost was finally formed at the end of the Holocene optimum, around 5000 to 3000 before present (Rasch, 2000). The geological history explains the typical stratigraphic profile encountered in Ilulissat, mainly consisting of silt and clay layers. Very ice-rich material (volumetric ice contents >50%) is often found below the permafrost table (Fig. 1b), and the ice content decreases with depth as the salinity increases to full seawater salinity (Tomaškovičová and Ingeman-Nielsen, 2023). Nowadays, the ALT generally ranges between approximately 0.3 m to 2.3 m (Scheer et al., 2023a). During the hydrological year 2018–2019, the mean annual ground temperature (MAGT) at borehole ILU2018–03 (Fig. 1a) was −2.2 °C at the depth of zero annual amplitude (ZAA, defined as the depth of maximum annual amplitude <0.1 °C) (Scheer et al., 2023b). Characterized as relatively warm and ice-rich, the permafrost is therefore very sensitive to natural and anthropogenic

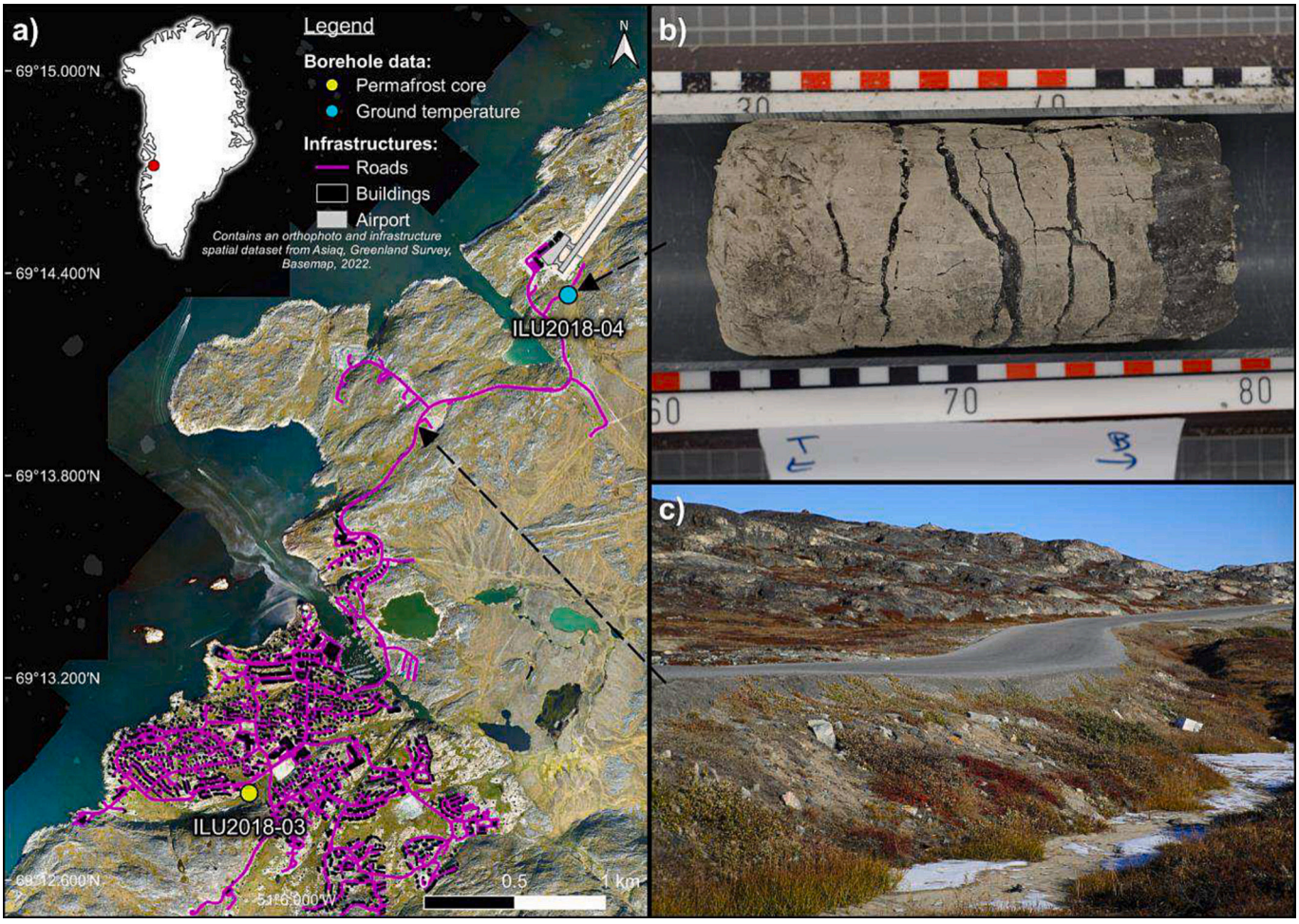

Fig. 1. Study area, local permafrost and infrastructure conditions. (a) Map of Ilulissat town area. The map contains an orthophoto and infrastructure spatial data from Asiaq, Greenland Survey, Basemap, 2022 (Asiaq Greenland Survey, 2022). (b) Permafrost core constituted of fine-grained material with thick and regularly oriented ice lenses, retrieved in one of the main sedimentary basins (borehole ILU2018–04). (c) Road crossing a sedimentary basin and affected by differential thaw settlements.

disturbances.

Ilulissat's landscape is relatively flat and described by an alternation of bedrock outcrops, fine-grained sedimentary basins, lakes and wetlands. Buildings are usually constructed on stable bedrock, while the road network (35 km long, as of January 1st, 2017, Statistics Greenland (2017)) stretches across the sedimentary basins (Fig. 1c). As evidenced by Scheer et al., 2023b, differential thaw settlements, induced by seasonal thawing and permafrost degradation, severely affect paved roads established on sediments and represent the main threat to the integrity of the road network. Furthermore, maintenance costs induced by permafrost thaw and climate change weigh on already tight municipal budgets, but are, to date, not systematically monitored (Scheer et al., 2023b). The stakeholders' capacity to implement adapted maintenance practices and take proactive measures to mitigate permafrost thaw is constrained by a lack of knowledge regarding local permafrost conditions, aggravated by a difficult access to existing data (Jungsberg et al., 2022; Scheer et al., 2023b). In this context, decision support tools are currently needed to maintain the road network serviceability and optimize resource allocation.

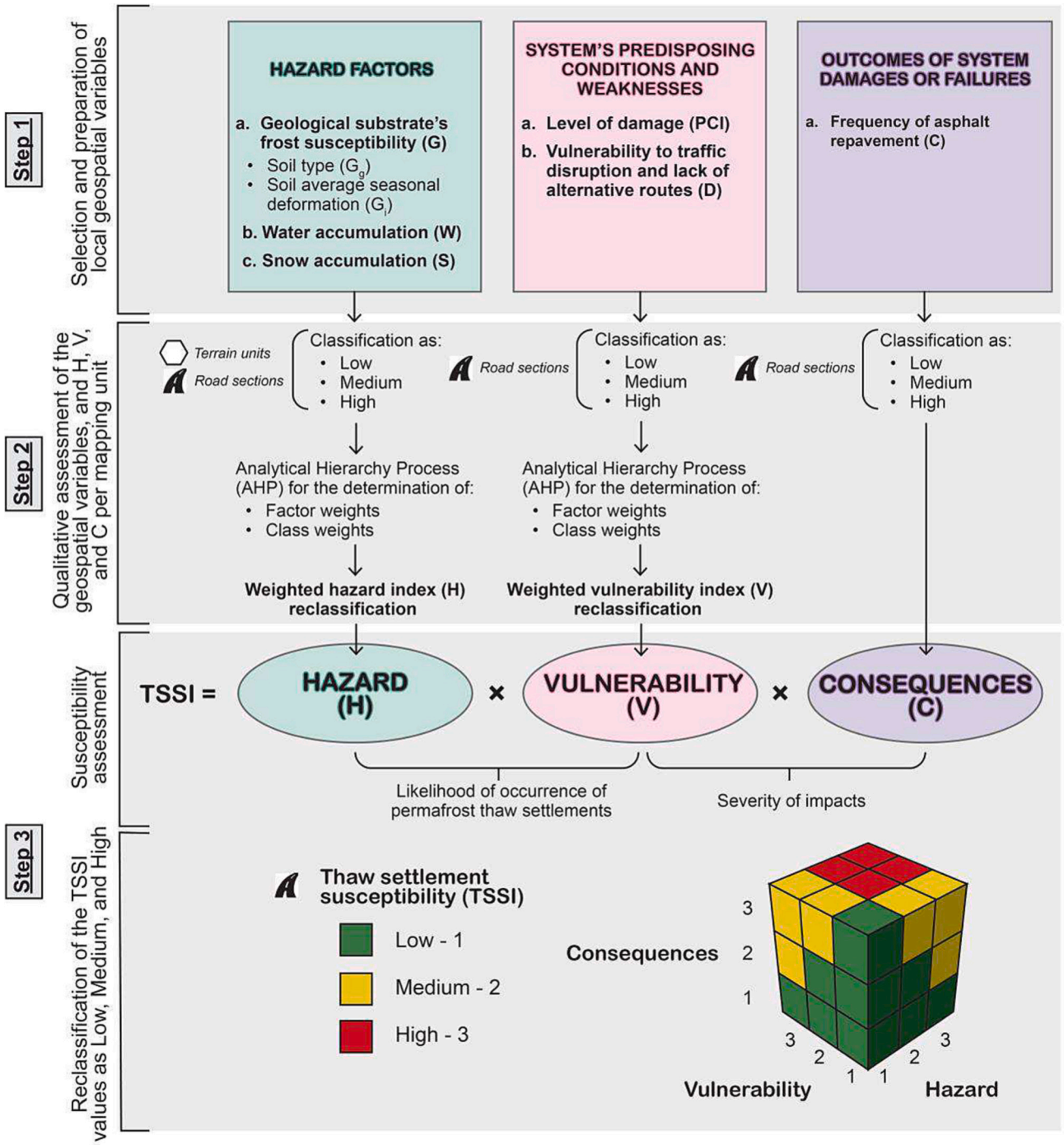

Fig. 2. Workflow diagram illustrating the computation steps of the Thaw Settlement Susceptibility Index (TSSI) for the case of Ilulissat, West Greenland. Geospatial data are gathered and combined to evaluate the different components of the TSSI, including hazard occurrences, current vulnerability of the system under consideration, and consequences. Applied to road networks, the framework enables a classification of road sections based on their susceptibility to permafrost thaw settlements.

3. Data and methods

A *Thaw Settlement Susceptibility Index* (TSSI) and mapping framework were developed to evaluate the physical, adaptive, and socioeconomic processes that would increase the susceptibility of roads to be impacted by permafrost thaw settlements. The formulation of the TSSI was designed to accommodate various environmental, infrastructural, and socioeconomic conditions encountered across different permafrost regions and communities. The following sections present the data, geospatial variables and methods combined and selected to compute the TSSI in the study area. The implementation steps of the TSSI assessment (Fig. 2) serve as a basis for reproducing or adapting the proposed framework in communities with similar or different challenges and datasets.

3.1. Geospatial datasets

To assess the susceptibility of the road network to thaw settlements in our study area, we combined existing geotechnical information with recent research outcomes comprising remotely sensed information and an infrastructure inventory. The technical characteristics of the datasets are presented in Table A.11, Appendix A.1.

3.1.1. Geotechnical data

Detailed maps of the surficial geology are currently not available in the area of Ilulissat. Historical borehole and shallow excavation logs — originating from site investigations conducted between the '60s and the '90s (Fig. A.11, Appendix A.2) — are currently stored as physical archives at Asiaq Greenland Survey. Despite providing precious information on the study area's permafrost conditions, the archives are not easily accessible to stakeholders from the construction and planning sectors. As part of this study, 56% of existing historical logs were digitized to characterize the road network's geological substrate and adjacent sedimentary basins. Geotechnical data (Scheer and Ingeman-Nielsen, 2023) obtained from contemporary site investigations were additionally compiled with the historical data to form a spatial database of ground properties. It is important to note that the surveyors involved over the years had variable geological knowledge and logging experience. Soil characterization errors and discrepancies may, therefore, occur in the spatial database of ground properties.

The digitized borehole stratigraphic profiles were then divided based on the presence or absence of fine-grained sedimentary layers within the first three meters below the ground surface (AL and top of permafrost). The borehole logs were, therefore, classified as fine- grained, versus coarse-grained (Fig. A.11, Appendix A.2). In the rest of the paper, we refer to the classification of the borehole logs based on the sediment grain size as *borehole classification*.

3.1.2. InSAR-derived thaw-season ground surface displacement map

Scheer et al. (2023a) processed Interferometric Synthetic Aperture Radar (InSAR) data covering thawing seasons 2015 to 2019 to identify frost-susceptible areas significantly affected by seasonal and long-term ground surface deformations. The average thaw-season ground surface displacement over the period of study was notably derived from the radar scenes with a 10 m nominal resolution and used in the present study.

3.1.3. Inventory of infrastructure conditions

An inventory of road conditions was carried out in Ilulissat in 2020 and 2021 by Scheer et al. (2023b). Road damages, repairs, and hazard factors potentially responsible for the deterioration of the road network were manually mapped and georeferenced in a Geographic Information System (GIS). Inputs retrieved from the inventory are summarized in Table A.11, Appendix A.1.

3.2. Thaw Settlement Susceptibility Index (TSSI) and mapping framework

3.2.1. TSSI

The TSSI and susceptibility mapping framework (Fig. 2) were based on the risk assessment models developed by Larsen et al. (2021), Duvillard et al. (2021), and Allard et al. (2023). The TSSI formula was derived from the engineering-based and probabilistic definition of risk (Faber, 2008; Lavell et al., 2012), expressed by Eq. 1 and corresponding to the product between the probability, P, of a harmful event to occur within a given time frame (hazard) and the consequences, C, associated with that event.

$$Risk = P \times C \tag{1}$$

Eq. 1 is nonetheless centered on the probabilistic characterization of the hazard and does not account for the socially-constructed and non-physical dimensions of risks (Larsen et al., 2021; Lavell et al., 2012). Based on those considerations and on the current need to holistically assess permafrost thaw risks (Larsen et al., 2021), we assimilated the TSSI to the risk formula proposed by Brooks et al. (2019), including the vulnerability of the studied system as an additional multiplicative component to Eq. 1.

The susceptibility of roads to permafrost thaw settlements, or TSSI, is therefore calculated as follows:

$$TSSI = H \times V \times C, \tag{2}$$

where H is the hazard level, or likelihood of permafrost thaw settlements occurrence and associated road failures within a given time frame, V is the road network's vulnerability to permafrost thaw settlements, and C are the consequences, or severity of permafrost thaw settlement impacts.

In the present study, the vulnerability of the road infrastructure contributes to increasing both the hazard likelihood and severity of the consequences. The multiplicative relationship between H, V and C, therefore reflects the non-linear and intertwined nature of those components and can be represented by a three dimensional matrix, as shown in Fig. 2. Using a matrix for the calculation of the TSSI is also compatible with the qualitative assessment of H, V, and C, remaining particularly relevant in Ilulissat and other remote Arctic communities where quantitative data are scarce.

3.2.2. Variables

An indicator-based approach was chosen to characterize the three components of the TSSI, H, V, and C. Six locally relevant variables, affecting the thaw settlement hazard levels, infrastructure vulnerability or consequence severity, were derived from the pre-processed geospatial datasets. Each of the variables introduced hereinafter was qualitatively classified as Low, Medium, and High per mapping unit (Fig. 2).

3.2.2.1. Hazard (H). Permafrost thaw settlement occurrences are driven by various natural and/or anthropogenic hazard factors. In this study, three hazard factors identified as a) the geological substrate's frost susceptibility (G), b) water accumulation (W), and c) snow accumulation (S) were used to characterize the likelihood of permafrost thaw settlements, H.

As previously mentioned, the ground ice content is one of the most important factors influencing the occurrence and magnitude of thaw settlements. However, characterizing the ground ice content and its distribution requires site investigations that are financially and logistically challenging in the Arctic. Due to the lack of detailed information regarding permafrost and soil properties in Ilulissat, we used the frost susceptibility of the ground as a proxy for the permafrost ice content. As clays and silts are particularly prone to the formation of ice in excess and occurrence of differential thaw settlements, they constitute the most frost-susceptible and hazardous sediment types (Andersland and Ladanyi, 2003; Allard et al., 2012; Ingeman-Nielsen et al., 2018). In comparison, coarse sediments, such as sands and gravels, are generally

characterized by lower ice contents (Allard et al., 2012), and thus, hazard levels. The local distribution of fine-grained deposits is therefore a first indicator of the geological substrate's frost susceptibility. Furthermore, areas annually affected by significant ground surface movements may be considered frost susceptible and hazardous for road embankments. For these reasons, we qualitatively assessed the substrate's frost susceptibility by combining the punctual information provided by the borehole classification of soil types, with the spatially continuous raster of thaw-season ground surface displacements.

The effects of water and snow on the ground thermal regime contribute to permafrost degradation (Doré and Zubeck, 2009; Scheer et al., 2023b). Scheer et al. (2023b) demonstrated that water and snow accumulations mapped in Ilulissat played important roles in the occurrence and/or aggravation of differential thaw settlements and pavement distresses. Consequently, these hazard sources were accounted for in the characterization of H.

3.2.2.2. Vulnerability (V). In the present study, we adopted the definition of vulnerability proposed by Berdica (2002) — "susceptibility to incidents that can result in considerable reductions in road network serviceability" — focusing on infrastructure potential level of damage and loss of serviceability. Two predisposing conditions contributing to thaw settlements were considered relevant in our assessment: a) the current level of pavement damage (*PCI*), and b) the vulnerability to traffic disruptions (*D*).

In Ilulissat, road sections impacted by thaw settlements in 2020 and 2021 exhibited severe pavement and structural failures due to the stresses exerted on the embankment. Ad-hoc repairs conducted on the road network were not always sufficient to mitigate or permanently solve such severe and perpetuating issues (Scheer et al., 2023b). For these reasons, we first hypothesized that the most vulnerable road sections to permafrost thaw settlements were most likely impacted by severe pavement distresses. Secondly, we presumed that the structural integrity of damaged road sections was already weakened and would continue deteriorating with further exposure to hazard sources. Based on these assumptions, the level of pavement damage (*PCI*) was derived from the infrastructure condition inventory to constitute the first indicator of the current road network's vulnerability, V.

Road failures induced by permafrost thaw hazards may also compromise access to essential facilities for the community, and necessitate emergency responses. The reduction or complete disruption of the road network's serviceability would impact daily lives and socioeconomic activities, thereby causing losses in resources. In the case of total traffic interruption, roads leading to critical infrastructures without alternative routes would be considered the most vulnerable to hazards and consequences and, thereby, the most important for the community. This is why, we secondly incorporated the vulnerability to traffic disruptions (*D*) into the evaluation of V.

3.2.2.3. Consequences (C). From an engineering perspective, assessing the severity of hazard consequences and infrastructure failures generally involves quantifying the repair costs and monetary losses associated with impairments and serviceability reductions (Brooks et al., 2019). In Ilulissat, the resurfacing of affected road sections is the primary coping strategy to lessen the impacts of permafrost thaw settlements and, thereby, is a recurrent source of expenses. However, due to the lack of systematic registration, available economic data did not allow associating specific costs to the management of permafrost-induced road damages (Scheer et al., 2023b). Given these limitations, repair costs could not be used directly in the computation of the TSSI. Instead, the repavement frequency over the period 2012–2021 was used as a proxy to evaluate the severity of thaw settlement consequences, C, on the road network.

3.2.3. Weighted hazard and vulnerability indices

Several factors contributing to H and V were previously identified. We used the Analytic Hierarchy Process (AHP) to assess the relative importance of each of these factors and determine weighted coefficients for the calculation of H and V. The AHP is a multi-objective and multi-criteria decision-making approach developed by Saaty (2008) and widely applied to resolve planning and geohazard mapping problems (Yalcin, 2008; Hong et al., 2014; Shahabi and Hashim, 2015; Hjort et al., 2018). The implementation of the method first requires to order each of the considered factors hierarchically, secondly to assign numerical values to expert judgements on the relative importance of each factor, and thirdly, to determine priorities to be attributed to these factors based on the synthesis of the judgements (Yalcin, 2008; Shahabi and Hashim, 2015). These steps corresponds to the creation of a reciprocal pair-wise comparison matrix, where each factor is rated against every other factor using a 9-point rating scale (Table B.12, Appendix B.1). When one factor on the vertical axis is considered equally or more important than the factor on the horizontal axis, a value ranging from 1 (equal importance) to 9 (extreme importance) is entered into the matrix cell. Conversely, each pair of reciprocals is given a value between 1/2 and 1/9. The consistency ratio (CR), formulated as follows, is calculated to evaluate expert judgement and ensure that the matrix was randomly generated.

$$CR = CI/RI \tag{3}$$

In Eq. 3, *RI* is the consistency index of a random-like matrix given by Saaty (1977) based on the order of the matrix, while *CI* is the consistency index of the evaluated matrix, expressed as:

$$CI = (\lambda_{max} - n)/(n-1), \tag{4}$$

where λ_{max} is the largest eigen value of the evaluated matrix and n is the order of the matrix. In principle, the AHP is applied for a set of criteria and decision-alternatives. In our study, the determination of priorities for the criteria is assimilated to the pair-wise comparison of the factors, while the ranking of decision alternatives, corresponds to the pair-wise comparison of the factors' sub-classes.

Three experts, with knowledge of the study area, jointly constructed reciprocal pair- wise comparison matrices for the hazard factors and their class values (Table B.13, Appendix B.2), and for the vulnerability factors and their class values, respectively (Table B.14, Appendix B.3). The consistency ratios of the different AHP models were calculated and the models were considered successful when CR was inferior to 0.1. The weighted hazard and vulnerability indices were finally obtained by multiplying the weight of each factor by its corresponding class weight.

For a given mapping unit i, the hazard index is therefore expressed as:

$$H(i) = w_G \times y_{G,j} + w_W \times y_{W,j} + w_S \times y_{S,j}, \tag{5}$$

where w_G, w_W and w_S are the weights attributed to the respective hazard factors, namely, the geological substrate's frost susceptibility, *G*, water, *W*, and snow accumulations, *S* (Table B.13, Appendix B.2). $y_{G,j}$, $y_{W,j}$, and $y_{S,j}$ correspond to the weights of the jth class value (low, medium, high) respectively taken by the hazard factors, *G*, *W*, and *S* (Table B.13, Appendix B.2) within the mapping unit.

Similarly, the vulnerability index is formulated as:

$$V(i) = w_{PCI} \times y_{PCI,j} + w_D \times y_{D,j}, \tag{6}$$

where w_{PCI} and w_D are the weights attributed to the respective vulnerability factors, namely, the pavement level of damage, *PCI*, and the vulnerability to traffic disruptions, *D* (Table B.14, Appendix B.3). $y_{PCI,j}$ and $y_{D,j}$ correspond to the weights of the jth class value (low, medium, high) respectively taken by the vulnerability factors, *PCI* and *D* (Table B.14, Appendix B.3) within the mapping unit.

Final values for the H and V components were retrieved per mapping

unit by reclassifying the hazard and vulnerability weighted indices according to the chosen qualitative scale.

The following parts of the paper describe the assessment scheme and computation steps of the TSSI undertaken in a GIS, for the case of Ilulissat.

3.3. Assessment scheme and computation of the TSSI

Considering the challenges generated by the maintenance of the road network in Ilulissat, we chose to assess the susceptibility of paved roads to permafrost thaw settlements for the period 2012–2021. The system considered in this study specifically consisted of 0.139 km^2 of paved roads (representing 67% of all paved roads in Ilulissat) established on sedimentary permafrost terrains. In order to ensure the practicality and readability of the susceptibility maps for local stakeholders (i.e., Avannaata municipality's Technical Department), the road network was divided into 506 coherent road sections of approximately 50 m in length, constituting the system's units under assessment. Road sections underlain by bedrock are out of the scope of this study and were discarded.

3.3.1. Hazard characterization

The frost susceptibility of the ground, water and snow accumulations influence the permafrost thermal regime and thaw processes not only underneath road embankments but also in their surroundings. Therefore, the entire study domain was spatially discretized into 50 by 50 m hexagonal terrain units (also referred to as *hexagonal cells*). Hazard levels associated with these factors were first evaluated within each hexagonal unit before being projected onto the predefined road sections.

3.3.1.1. Frost susceptibility (G). Two complementary datasets were used to assess the frost susceptibility of the geological substrate and its predisposition to thaw settlements, *G*. Fig. 3 illustrates the overall workflow followed to combine the datasets and classify each terrain unit of the study domain.

We started by characterizing the hazard levels associated with different soil types, ranging from low, for stable bedrock outcrops, to high, for fine-grained sediments. The soil type hazard levels, referred to as *Gg*, were evaluated for each hexagonal unit (Fig. 4) based on: i) the land cover classification, ii) geotechnical data availability and density, iii) soil type classification of borehole logs.

The land cover classification was used as a first level of screening to identify terrain units predominantly underlain by bedrock and assumed to be stable. A low hazard level was assigned to hexagonal cells, with at least two-thirds of their surface covered by bedrock outcrops (Fig. 4, step a).

The next steps of the assessment consisted in extrapolating the borehole log classification and determining the soil types of the remaining hexagonal cells underlain by sedimentary deposits. Three case scenarios, identified based on the availability of geotechnical data per terrain unit, conditioned each step of the evaluation scheme. Firstly, provided that geotechnical data were available within a given cell (Fig. 4, step b), the soil type could be inferred, and the corresponding hazard value attributed. In this scenario, referred to as case 1, we calculated the percentage of borehole logs classified as fine-grained within the cell. As the surficial soil type distribution may be spatially variable across a sedimentary basin, the borehole classification may also indicate punctually contradicting information over a small area. For this reason, when 20% or more of the borehole logs indicated the presence of fine-grained deposits within the cell (Fig. 4, step c), the likelihood of thaw settlements with respect to the soil type was considered high within that cell. Otherwise, and if more than one borehole log was classified as coarse, the hexagon terrain unit was assumed to be predominantly coarse and assigned a medium hazard level (Fig. 4, step d).

Secondly, geotechnical data were sometimes unavailable within a given cell (case 2). If neighboring terrain units could be classified based on their soil type, the highest hazard value encountered across the six neighboring units was attributed to the central cell under consideration (Fig. 4, step e).

Thirdly, in the last scenario (referred to as case 3), geotechnical data were unavailable within the considered terrain unit (Fig. 4, step b) and neighboring cells (Fig. 4, step e). When the soil type of the terrain unit could not be inferred, a medium hazard value was assigned by default as a precaution.

After evaluating the soil type hazard levels across the study domain, the ground surface displacements measured by InSAR were considered. The pixels of the seasonal displacement raster were averaged within each hexagonal terrain unit. The hazard levels associated with the average seasonal ground surface displacement and referred to as *Gi*, were assessed from low to high according to Table 1.

Finally, based on the values taken by G_g, and G_i in the three case scenarios, the permafrost thaw settlement likelihood inherent to the

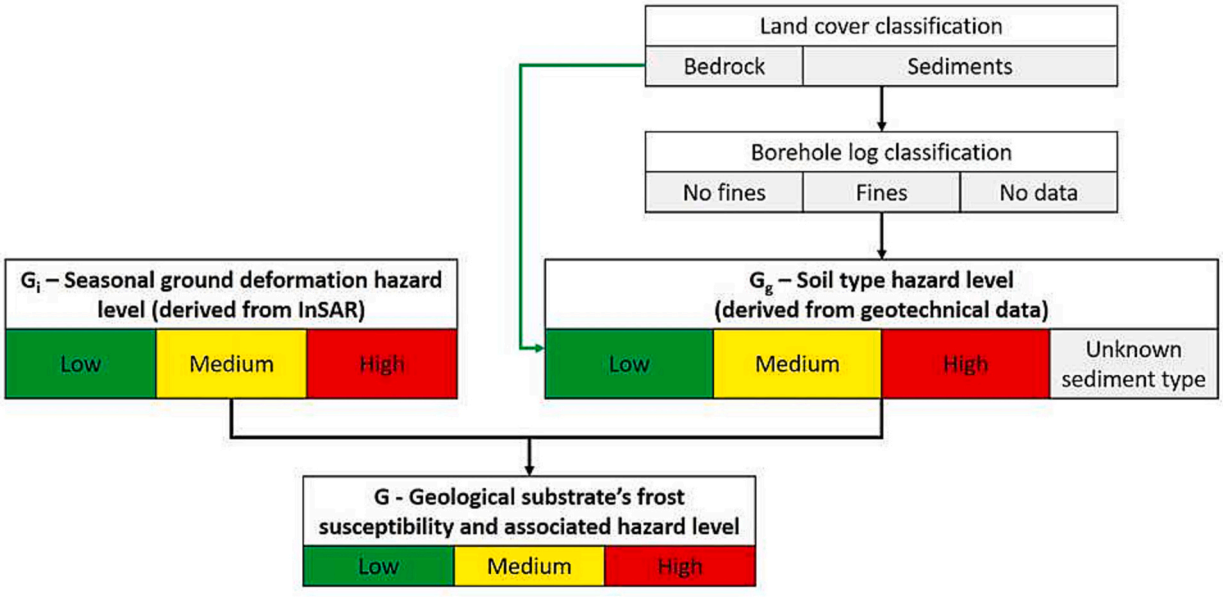

Fig. 3. Assessment of the hazard levels, *G*, inherent to the geological substrate's frost susceptibility.

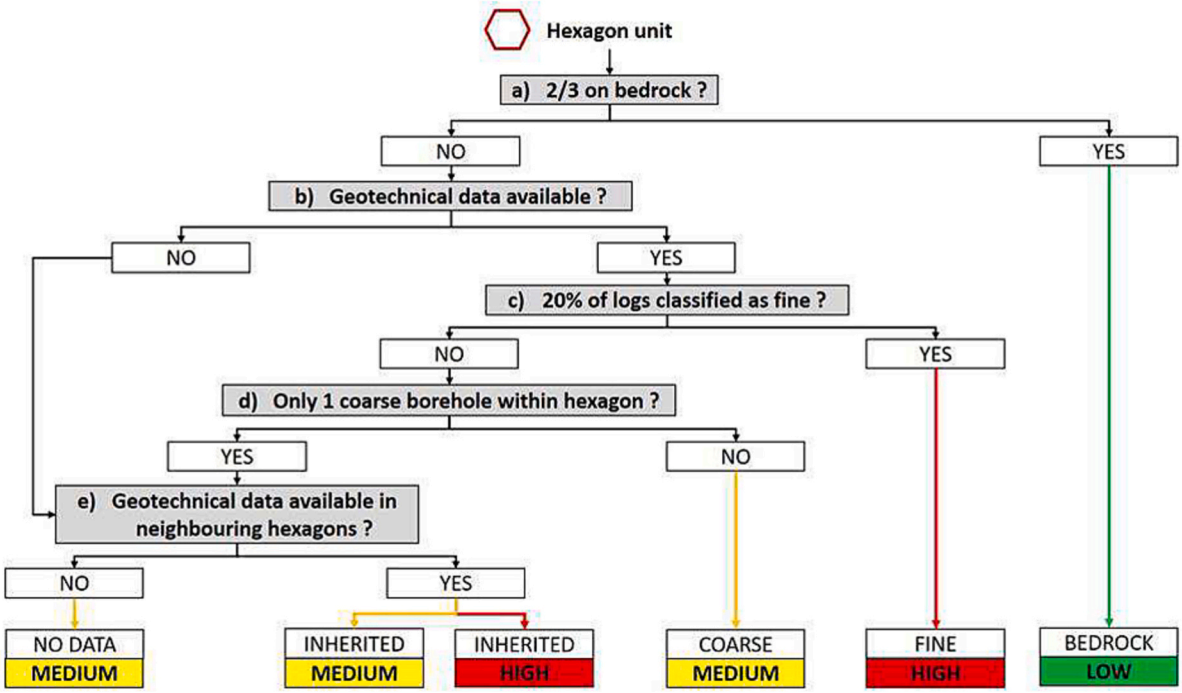

Fig. 4. Evaluation scheme of the soil type hazard levels, G_g, based on the land cover and borehole classification, and availability of the geotechnical data.

Table 1
Evaluation scheme of the hazard levels, G_i, associated with InSAR-derived average seasonal ground surface displacement (over the period 2015–2019).

InSAR average seasonal surface displacement [m]	Ground surface displacement hazard level (G_i)
> -0.005	Low
> -0.01 and ≤ -0.005	Medium
≤ -0.01	High

frost susceptibility of the geological substrate was determined.

In case 1, when both G_g and G_i were classified as medium or high, the maximum value between the two indicators was retained as the final hazard level, G (Table 2). G levels were only lessened with respect to G_g and G_i, when remotely sensed averaged ground displacements were negligible (G_i evaluated as low), or the soil substrate was evaluated as non-frost susceptible (G_g evaluated as low).

In case 2, G_g values were then inherited from neighboring units whose predominant soil type could be determined. For this reason, final G values, derived from G_g and G_i, were evaluated similarly to case 1 (Table 3). The contribution of G_i prevailed over the soil type information G_g only when measured average surface displacements were classified as

Table 2
Assessment of the hazard levels, G, inherent to the geological substrate's frost susceptibility, based on the values of G_g and G_i when geotechnical data are available.

Case 1: Geotechnical data available G – GEOL. SUBSTR. HAZARD LEVEL		G_g – Soil type hazard level	
		Medium	High
G_i – Seasonal ground deformation hazard level	Low	Low	Medium
	Medium	Medium	High
	High	High	High

Table 3
Assessment of the hazard levels, G, inherent to the geological substrate's frost susceptibility, based on the values of G_g and G_i when geotechnical data are available.

Case 2: Geotechnical data inherited G – HAZARD LEVEL		G_g	
		Medium	High
G_i	Low	Medium	Medium
	Medium	Medium	High
	High	High	High

Table 4
Assessment of the hazard levels, *G*, inherent to the geological substrate's frost susceptibility, based on the values of G_i when geotechnical data are unavailable.

Case 3: No data / Unknown sediment type G – HAZARD LEVEL		G_g
		Medium
G_i	Low	Low
	Medium	Medium
	High	High

Table 5
Qualitative classification of water accumulation hazard levels, *W*.

Water accumulation level	Water accumulation hazard level (*W*)
Absence	Low
Superficial water ponding and ditches with residual stagnant water	Medium
Significant water ponding, wetlands, streams, and ditches with stagnant water	High

Table 6
Qualitative classification of snow accumulation hazard levels, *S*.

Snow accumulation level	Snow accumulation hazard level (*S*)
Absence or minor lateral snow ploughing	Low
Significant lateral snow ploughing	Medium
Significant snow piling	High

low.

Finally, in case 3, final *G* levels, consequently, relied on the remote-sensing information and took the values of G_i (Table 4).

3.3.1.2. Water (W) and snow (S) accumulations. Water accumulations (*W*) registered in the surroundings of road embankments were categorized as illustrated in Table 5. Superficial water ponding and residual stagnant water observed in artificial drainage systems were assigned a medium hazard class. The thaw settlement likelihood was considered the greatest in areas characterized by the presence of wetlands, streams, and significant water ponding.

Similarly, hazard levels were assigned based on the qualitative classification of winter snow deposits resulting from snow removal operations. Lateral snow ploughing is needed in Ilulissat throughout the winter season as snow precipitations may be important. However, in some areas, snow has to be more heavily accumulated laterally due to wind drifts or the impossibility of gathering snow on both sides of the road. The snow-insulating action was assumed to be more hazardous in this case (Table 6). Finally, preferential zones for snow piling, located on sensitive sedimentary terrains, were the most likely to show signs of differential thaw settlements and induced road damages (Scheer et al., 2023b).

3.3.1.3. Final hazard levels (H). Hazard levels were calculated by applying Eq. 5, with the factor and class weights summarized in Table Appendix B.2, Appendix B.2, to all the hexagonal terrain units of the study domain. Natural breaks resulting from the Jenks optimization method (Jenks, 1967) were used to divide the obtained H values into the three classes, defined as low, medium, and high.

The H values of the hexagonal terrain units overlapping with the road network were reprojected onto the predefined 50 m road sections.

Fig. 5. Example of predefined road section established onto terrain units characterized by hazard values. Low, medium, and highly hazardous segments represent respectively, 39, 55, and 6% of the road section. The highly hazardous segment is negligible in coverage; therefore, the entire road section was attributed a medium hazard level.

A given road section may be underlain by several terrain units characterized by different hazard levels (Fig. 5). Hence, the surface areas of the road's low, medium, and highly hazardous segments were calculated, and their percentage relative to the total area of the road section was retrieved. A segment covering >15% of the section's total area was considered significant, and its H value was taken into consideration. As a principle of precaution, if the road section was divided into two or three significant segments with different H values, the maximum hazard value encountered across the segments was allocated to the entire section (Fig. 5).

3.3.2. Road network's current vulnerability

Assessing the factors conditioning the vulnerability of the road network constituted the second step in the susceptibility mapping. The infrastructure level of damage, *PCI*, providing information about weakened embankments and road sections prone to further deterioration, and the vulnerability of the roads to traffic disruptions, *D*, were individually classified as follows.

3.3.2.1. Level of damage (PCI). The inventory of pavement distresses, and their severity levels were firstly used as inputs to calculate a Pavement Condition Index (PCI) for each road section. The PCI is a numerical rating widely used by entities in charge of transport infrastructure and operations to monitor pavement conditions (ASTM International, 2008). The index indicates the state of the road surface at the time of observation and ranges from 0 to 100, with 0 being the worst possible condition. We first adapted the ASTM procedure (ASTM International, 2008) to our system by excluding or including pavement distresses typically encountered on permafrost terrains and not described by the standard. For instance, differential thaw settlements were assimilated to depressions, and tension cracks to longitudinal cracks. In order to reflect the destabilization and collapses of the embankment slopes in the PCI, we included such failures as severe edge cracking. The extent of each distress type was then retrieved per road section, and we finally computed PCI values using the algorithm by Monroe (2017). The PCI values generated by the algorithm were validated against PCI values calculated manually on 10 randomly chosen road sections following the ASTM procedure (ASTM International, 2008).

The obtained PCI values were categorized into three classes (Table 7) representing the severity of the pavement damages.

Table 7
Qualitative classification of road vulnerability based the assessment of pavement conditions.

PCI value	Level of damage (*PCI*)
>55 and ≤ 100	Low
>25 and ≤ 55	Medium
≤ 25	High

3.3.2.2. Traffic disruptions and alternative routes (D). We secondly characterized the road sections based on their importance for the community and on the existence of alternative routes in the event of traffic disruptions. To this aim, we used the Python package NetworkX (Hagberg et al., 2008) to analyze possible routes between a set of start and destination points. Road center lines (derived from the TBM, Asiaq Greenland Survey, 2022) were used as input to generate a multigraph of nodes and edges representative of Ilulissat's roads and intersections. Among the nodes, 18 infrastructures considered critical for the community (e.g., airport, hospital, power plant, etc.) were defined as destination points. All dead ends and road intersections were then extracted as 902 start points (different from the destination points). Each edge of the multigraph was iteratively removed to represent the total loss of serviceability of each road section. The shortest paths between the start and destination points were computed at each iteration using the Dijkstra algorithm (Dijkstra, 2022). Alternative routes to the disrupted road section did not exist when the shortest path between a start and destination point could not be computed. On this basis, we counted how many times removing an edge from the multigraph resulted in the impossibility of generating routes between the set of start and destination points, as illustrated in Fig. 6. All edges of the road network were classified based on these values using the three-class system presented in Table 8.

We finally reprojected the values of *D* resulting from the network analysis, onto the predefined road sections. If a road section was characterized by two or three different *D* values, the road section was given the value of the most prominent class in coverage relative to the section's total area. In the case where the road section was equally divided into two segments with different *D* values, the lowest value was attributed to the road section. Otherwise, if a road section was characterized by three different *D* values covering less than 50% of the section, the section was attributed a medium class.

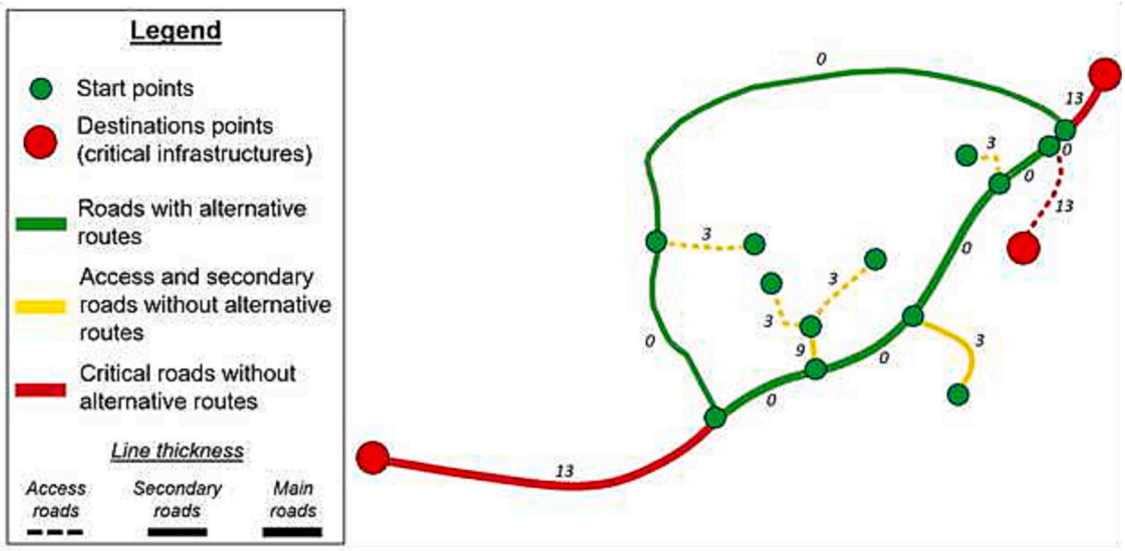

Fig. 6. Example of road sections classified based on the existence of alternative routes in the event of traffic disruptions. The figure shows the results that would be produced by the algorithm with a set of 13 start points and 3 destination points. The numbers represent how many times the loss of serviceability of the respective road sections resulted in the impossibility of computing the shortest routes between the start and destination points.

Table 8
Qualitative classification of road vulnerability based on the existence of alternative routes to traffic disruptions. Corresponding road types are described according to the "Level of traffic" classification used in the infrastructure inventories of Scheer et al. (2023b).

Count	Typical road sections	Vulnerability to traffic disruptions (*D*)
0	Roads (incl. access, secondary and main roads) with alternative routes	Low
≥ 18 and ≤ 468	Access and secondary roads serving residential areas (start points), without alternative routes	Medium
≥ 901	Roads (incl. access, secondary and main roads) serving critical infrastructures (destination points), without alternative routes	High

3.3.2.3. Final vulnerability levels (V). Vulnerability levels were calculated by applying Eq. 6, with the factor and class weights summarized in Table B.14, Appendix B.3, to all the road sections. Jenks natural breaks (Jenks, 1967) were lastly used to reclassify the obtained vulnerability values as low, medium and high.

3.3.3. Consequence severity (C)

On permafrost terrains, repavement may be needed overall every 3 to 4 years, against 13 to 15 years in the absence of permafrost (Doré et al., 2022). Using the inventory of repavement cycles, we counted the number of asphalt layovers that had been applied to each road section since 2012 and classified them according to Table 9. Road sections repaved twice within less than three years were assumed to be severely affected by permafrost thaw settlements and to necessitate more resources on a regular basis.

3.3.4. Calculation of the TSSI

The classes low, medium, and high of the H, V, and C components were attributed corresponding integer scores ranging from 1 to 3, to facilitate the computation of the TSSI in the GIS. The TSSI was ultimately calculated with Eq. 2 for each road section. Susceptibility levels resulting from the multiplication of H, V, and C were obtained from the 3D matrix represented in Fig. 2, and reclassified according to Table 10.

Boundaries between the TSSI classes were determined based on the knowledge of the study area and remaining uncertainties associated with permafrost conditions and contribution of hazard sources to thaw settlements. Stakeholders' perceptions and concerns with respect to road maintenance challenges and incurred costs also motivated our choice to reclassify TSSI values above 4 as medium and high.

In this way, road sections with a high susceptibility to hazardous factors which have not been extensively repaired or damaged during the study time frame, may still be moderately or highly susceptible to thaw settlements. On the contrary, road sections that have been extensively damaged and repaired but are neither established on frost susceptible sediments nor in the vicinity of hazardous factors may be adversely affected by other processes beyond the scope of this study. The TSSI should consequently be low or medium.

Table 9
Qualitative classification of road repair severity, C.

Frequency of repavement over the period 2012–2021	Severity of the consequences (C)
Never repaved	Low
Repaved once, or repaved twice in 2012 and 2019	Medium
Repaved twice in 2019 and 2020	High

Table 10
Reclassification scheme of the thaw settlement susceptibility index (TSSI).

Result of the multiplication of H, V, and C	Final TSSI value
≥ 1 and ≤ 4	Low
≥ 6 and ≤ 9	Medium
≥ 12 and ≤ 27	High

4. Results

4.1. AHP

Ground ice content was ranked by the group of experts as the primary determinant in the occurrence and magnitude of thaw settlements in Ilulissat. For this reason, a weight of 0.75 (Table B.13, Appendix B.2) was attributed to the frost susceptibility of the geological substrate, *G*, serving in our study as indicator of the amount of ground ice (Table Appendix B.2, Appendix B.2). Some authors have considered the effect of snow as one of the most critical in the susceptibility of terrains to permafrost degradation and thaw settlements (Hong et al., 2014). However, based on the results of Scheer et al. (2023b) who showed that at least 60% frost-related road damages occurred in areas affected by poor water drainage in Ilulissat, we allocated a higher weight to the effects of water accumulations. Road conditions were surveyed by Scheer et al. (2023b) at the end of the summer season. Since the study area is relatively flat, the authors assumed that the melting of significant snow deposits may have contributed to water ponding issues, especially where artificial drainage systems were disrupted. Coefficients of 0.15 and 0.10 were, therefore, respectively applied to *W* and *S* (Table B.13, Appendix B.2). Higher weights (ranging from 0.58 to 0.76) than for the classes "Low" and "Medium" were finally attributed to the class "High" of each hazard factor (G, W, and S).

Table B.14 in Appendix B.3 summarizes the weighted coefficients that were obtained from the AHP to compute the weighted vulnerability index per road section. Based on local knowledge, total interruptions of the traffic had never occurred in Ilulissat over the last decade, due to permafrost hazards. For this reason, we attributed more weight to the level of damage (0.67) than the vulnerability to traffic disruptions (0.33). Based on expert judgements, medium and high *PCI* classes contributed more importantly to road sections' vulnerability, and were therefore given weights of 0.35 and 0.58, respectively. Roads without alternative routes and leading to critical facilities in the community (high *D* class) were weighted with a coefficient of 0.74 in the calculation of the vulnerability index.

4.2. Spatial distribution of the hazard factors

Fig. 7 shows the hazard levels inherent to the frost susceptibility of the geological substrate. The map 7a first illustrates the distribution of the different soil types (G_g) derived from the land cover classification and extrapolated borehole information (Fig. A.11, Appendix A.2). Red areas represent frost susceptible sediments, such as silts and clays, which contain ice and result in differential thaw settlements. These terrain units underlay approximately 59% of the road network. In comparison, 6 and 12% of the roads were established in areas respectively classified as coarse-grained and unknown sediments. The remaining 23% of the road network was constructed on stable bedrock outcrops.

Fig. 7b secondly represents the average magnitude of seasonal ground surface displacement measured by InSAR for the period 2015–2019 and classified per hazard level (G_i). Red hexagonal units, underlying 15% of the road network, were affected by significant seasonal downward movements and were, as a result, considered highly hazardous for roads. In comparison, 53% of the road network was established on stable (non-frost-susceptible) terrain units, according to the remote-sensing data.

Final hazard levels, *G*, associated with the geological substrate's frost

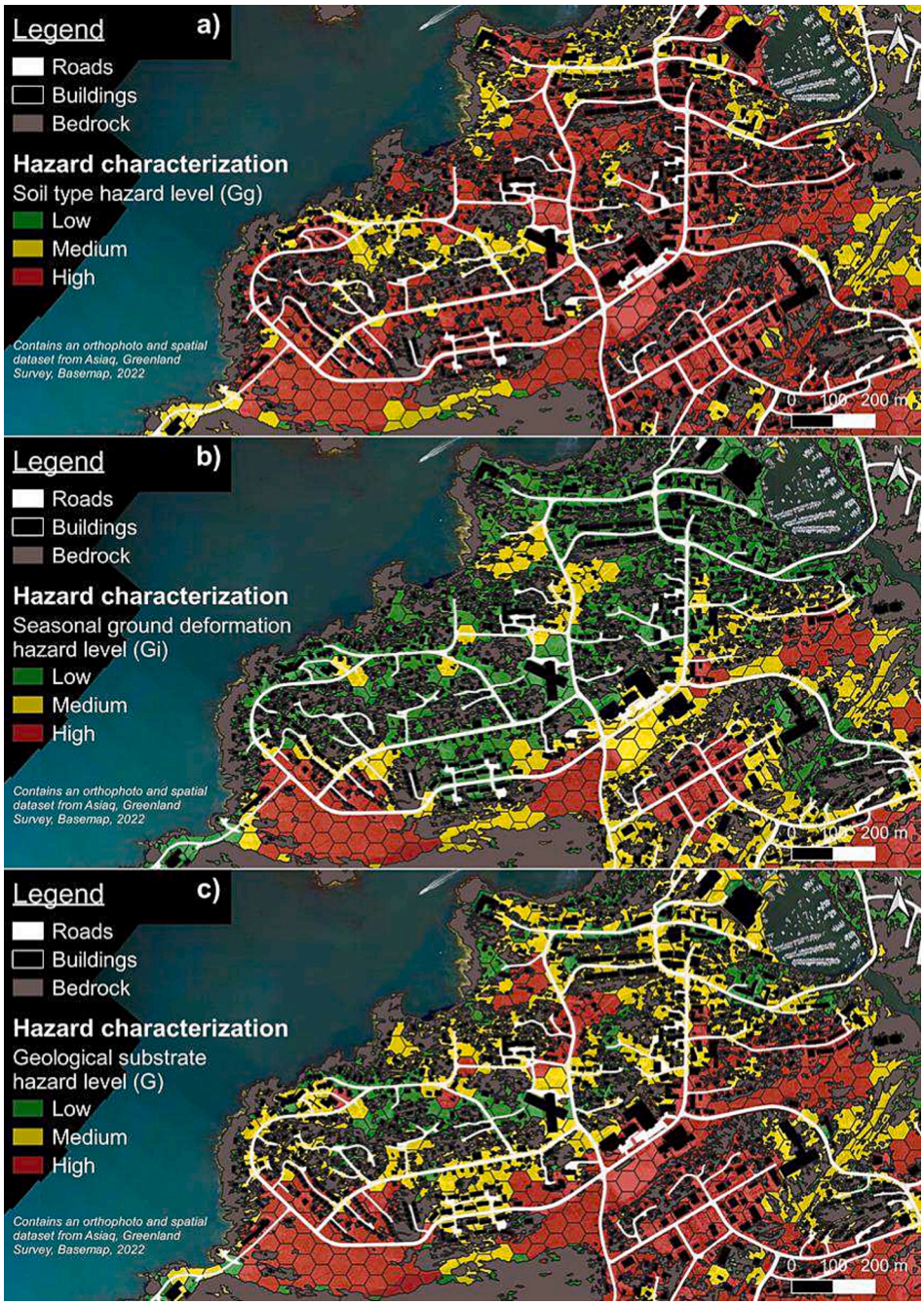

Fig. 7. From top to bottom: (a) soil type distribution and associated hazard levels (G_g), (b) InSAR-derived average seasonal ground displacement for the period 2015–2019, classified per hazard level (G_i), and (c) final hazard levels, G, derived from G_g and G_i and associated with the geological substrate's frost susceptibility. The maps contain an orthophoto and spatial data from Asiaq, Greenland Survey, Basemap, 2022 (Asiaq Greenland Survey, 2022).

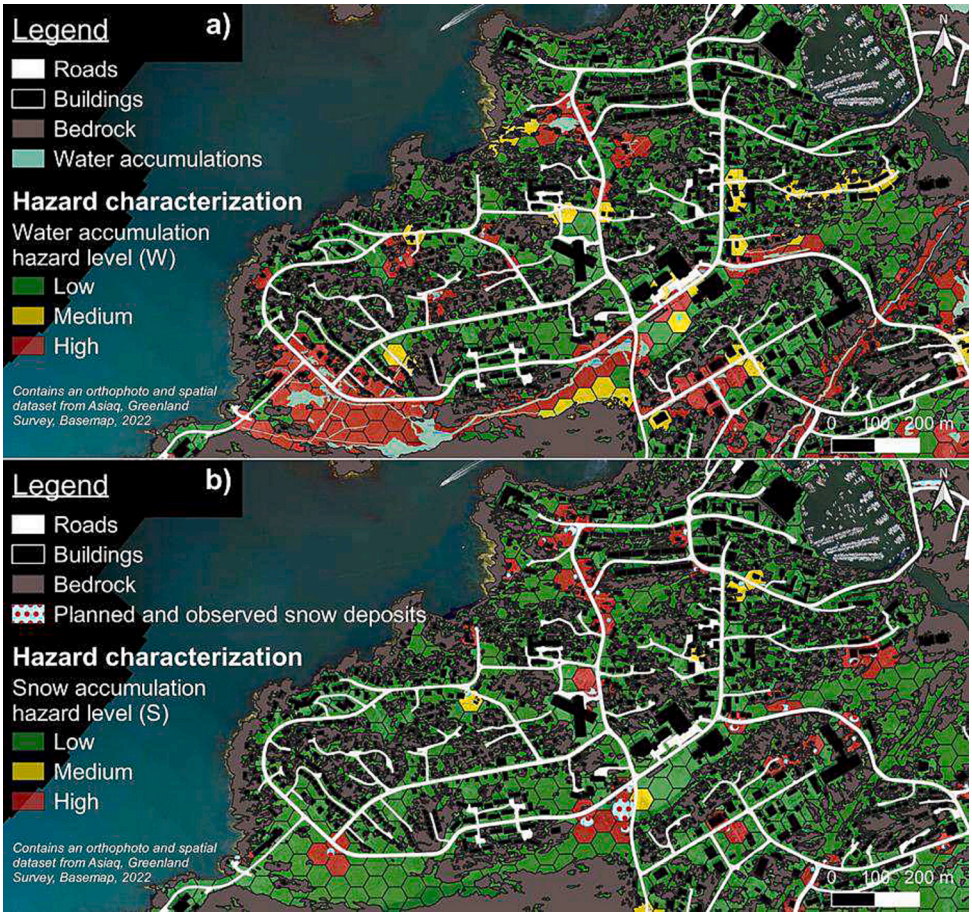

Fig. 8. From top to bottom: (a) geological substrate's frost susceptibility, (b) water accumulation (W), and (c) snow accumulation (S) hazard maps. The maps contain an orthophoto and spatial data from Asiaq, Greenland Survey, Basemap, 2022 (Asiaq Greenland Survey, 2022).

susceptibility and based on the combination of the geotechnical (G_g) and remote-sensing information (G_i), are shown in Fig. 7c. In the end, 33% of the road network was established on frost susceptible substrate with a high predisposition for thaw settlements. Furthermore, respectively, 16 and 9% of the roads were assessed as highly hazardous due to poor water drainage and snow accumulations, as illustrated in Fig. 8.

The probability of occurrence of permafrost thaw settlements, resulting from the weighting of the three hazard sources, *G*, *W* and *S*, by AHP, is shown for the road network and its surrounding environment in Fig. 9a. Thaw settlements are the most likely to occur or to have occurred on the road sections highlighted in red. Respectively, 33 and 39% of the assessed road surface area were evaluated as moderately and highly hazardous. At these locations, the geological substrate's properties, water, and snow accumulations individually or concomitantly influenced the occurrence and magnitude of thaw settlements and posed a risk to road embankments. Drainage and snow ploughing practices may notably need to be improved to lessen the effects of water and snow on the permafrost regime.

4.3. Impacted and vulnerable road sections

Fig. 9b highlights the road sections where thaw settlements have already impacted the pavement layer and embankment structural integrity, requiring frequent repairs. The severity of thaw settlement-induced impacts, evaluated based on the repavement frequency, was moderate and high for respectively, 35 and 3% of the assessed road surface area.

The road axes depicted in red in Fig. 9c and representing 9% of the assessed road surface area, are considered particularly vulnerable to permafrost thaw settlements due to the current level of damage, and lack of alternative routes to ensure the accessibility to critical infrastructures in the event of traffic disruptions. These two factors, contributing to the vulnerability of the road network, are individually mapped in Fig. C.12, Appendix C. In total, around 6% of the assessed road surface area presented a high potential for damage. The deterioration of severely damaged road sections will plausibly continue as permafrost degrades and ground ice melts. In comparison, around 12% of the roads leading to critical facilities and without alternative routes were evaluated as essential for the community of Ilulissat and, thereby, as particularly vulnerable to traffic disruptions and total loss of serviceability.

4.4. Road network thaw settlement susceptibility

The final TSSI values based on the multiplication of H, V, and C are illustrated in Fig. 10. Overall, 22 and 12% of the assessed road surface area were moderately and highly susceptible to permafrost thaw settlements at the time of the study (2012−2021). The roads concerned by such high TSSI values stretched across the main sedimentary basins in Ilulissat, which were predominantly frost-susceptible, and often affected by poor water drainage caused by the gentle topography and melting of ice-rich permafrost. Piling snow on such terrains and in the close vicinity of embankments constitutes a risky practice that may further disturb the permafrost regime and aggravate water impoundment issues. These road sections are therefore expected to require more effort and resources from the municipal Technical Department to maintain their serviceability.

The TSSI values of some residential and secondary road sections nonetheless seemed to have been overestimated. This result could be explained by uncertainties in the geological substrate conditions or very

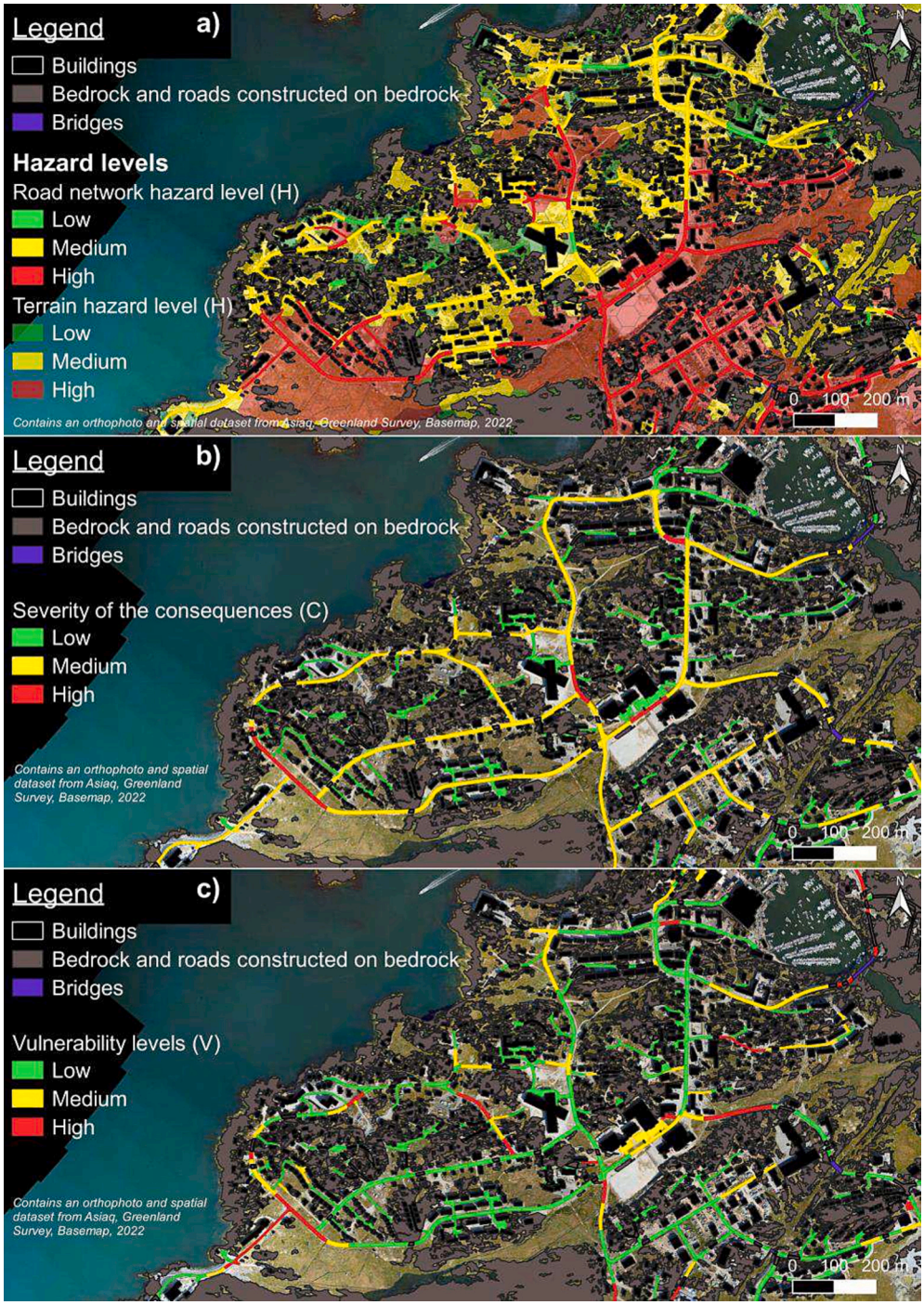

Fig. 9. From top to bottom: (a) levels of hazard, (b) severity of consequences (C), and (c) vulnerability (V) currently characterizing Ilulissat's road network. The maps contain an orthophoto and spatial data from Asiaq, Greenland Survey, Basemap, 2022 (Asiaq Greenland Survey, 2022).

Fig. 10. Thaw settlement susceptibility map (2012–2021) of Ilulissat's road network. The map contains an orthophoto and spatial data from Asiaq, Greenland Survey, Basemap, 2022 (Asiaq Greenland Survey, 2022).

poor pavement conditions of these sections, increasing the hazard and vulnerability levels and by extension the TSSI. Such outcomes do not affect the applicability of the map whose aim was to support the prioritization of road maintenance operations and optimization of local resources. Furthermore, looking at the individual values taken by H, V, and C facilitates, in these scenarios, the interpretation of the TSSI and comprehension of the road conditions. Finally, these results also represent valuable insights to fine-tune the site-specific classification scheme and weighted coefficients used for the assessment of the TSSI.

5. Discussion

This study addressed the need for more comprehensive assessments of permafrost hazards and risks at the local scale (Duvillard et al., 2021; Doré et al., 2022; Hjort et al., 2022). From a planning and engineering perspective, the challenges in building and maintaining infrastructures on sensitive permafrost terrains often resides in the lack of knowledge regarding local permafrost properties and hazards, or in the difficulty to gather relevant information. Limited logistical and financial resources additionally constrain the possibility of conducting detailed site investigations in remote Arctic regions. However, optimal risk and infrastructure management also rest upon our ability to collect, extrapolate and combine local knowledge and already existing data, meaningfully and practically.

Focusing on the susceptibility of transportation infrastructure to thaw settlements, we developed a mapping framework presenting the advantage of being easily adaptable to local conditions, needs, resources, and data availability. The framework was specifically designed to assess: i) environmental and anthropogenic hazard sources, ii) factors contributing to infrastructure vulnerability to permafrost thaw and hazards, and iii) socioeconomic impacts of infrastructure serviceability disruptions and failures.

We implemented the framework for the case of Ilulissat, West-Greenland, and demonstrated its potential in identifying road sections susceptible to permafrost thaw settlements. The TSSI maps were validated through field observations and consultation meetings conducted subsequently to the period of study, in October 2023. Most of the road sections evaluated as highly susceptible to permafrost experienced significant differential thaw settlements and repavement operations during the summer seasons of 2022 and 2023. Mapping the ground ice content distribution and geotechnical data availability was additionally considered very relevant to the local stakeholders from the construction and planning sectors, being currently confronted with a lack of and challenging access to information regarding soil properties. We successfully addressed this need by digitizing historical and recent data and using proxies to estimate the ground ice content. Despite insufficient economic records to assess the severity of various consequences from permafrost- induced road damages, we identified the most impacted and resource-consuming road sections by analyzing the repavement frequency based on stakeholders' inputs (Scheer et al., 2023b). Finally, the strength of the TSSI implementation resided in the synergistic use of a standard procedure for the determination of paved road conditions (ASTM International, 2008) and innovative network analysis algorithm to assess the current vulnerability of the road network. Our study specifically illustrated ways to gather and combine available data sources, such as borehole log archives, infrastructure inventories, and remote

sensing, in order to address local needs and challenges.

Compared to large-scale and pan-arctic studies (Nelson et al., 2002; Hjort et al., 2018; Streletskiy et al., 2019), which are relatively preoccupying regarding the fate of linear infrastructure on permafrost, our assessment showed that only a small portion of the road network is currently affected by and susceptible to permafrost thaw settlements in Ilulissat. Global models are important to raise general awareness but may overestimate the percentage of infrastructure at risk, notably due to their coarse resolution and inability to capture site-specific variations. Besides, low percentages of permafrost thaw-susceptible infrastructures still represent significant maintenance challenges and costs for communities with limited resources, especially in a context of increasing socio-environmental pressures. Therefore, mapping the current susceptibility of infrastructures to thaw settlements at the local scale remains needed to inform infrastructure maintenance and resource allocation.

Concerning the datasets used in our study, the registration of infrastructure damages, water, and snow accumulations was conducted with a simple methodology, aimed to be reproducible by stakeholders (Scheer et al., 2023b). Nonetheless, these observations were partly dependent on the timing and conditions of the surveys. Yearly and systematic in- situ monitoring of the interactions between the road embankments and hazardous processes will be needed to enhance the assessment of the hazard sources. Furthermore, as evidenced by Chai et al. (2018), pavement age, embankment designs and geometry influence the permafrost thermal regime and condition damage occurrences. More detailed information on engineering designs and construction standards implemented in Ilulissat and Greenland is generally needed. Particular attention should be given to embankment heights and structural layer properties. Finally, as hydrological and soil moisture regimes are evolving, a detailed investigation of the artificial drainage system's design and capacity to respond to seasonal and long-term climate changes would also contribute to improve the characterization of the infrastructure hazard potential (Doré et al., 2022; Hjort et al., 2022).

In order to compute the TSSI, we firstly discretized the study domain and road network in terrain units and road sections of 50 m. The size of the assessed system's units was chosen considering the density and availability of the geospatial datasets and with the aim to ensure the practical use of the TSSI maps for risk management and resource optimization. However, the discretization of the study domain (size and position of the grid cells) and sectioning of the road network may affect the classification of the road sections. Even though the most susceptible areas to thaw settlements would remain largely unchanged, the influence of the unit size on the geotechnical data extrapolation and TSSI values should be determined.

We secondly used the AHP to assess the relative importance of factors conditioning the likelihood of thaw settlements and infrastructure vulnerability. Despite the AHP proving effective in our study and previous geohazard research (Yalcin, 2008; Shahabi and Hashim, 2015), the rating process is based on expert judgement which may be considered subjective. A sensitivity analysis needs to be conducted to assess the percentage change in the final TSSI values when changing the weighted coefficients used in the hazard and vulnerability indices. The mapping framework presented here could, additionally, be enhanced by incorporating different statistical models or evaluation techniques. As data availability, permafrost and socioeconomic conditions significantly vary across the Arctic, choosing the right method to assess H, V, and C needs to be adapted at the local scale. However, while the weighted coefficients and classification thresholds used in this study remain site-specific, the proposed framework can still serve as standard approach for various permafrost environments.

Lastly, a detailed socioeconomic analysis of the impacts of infrastructure failures and disruptions will be necessary to move from mapping the thaw settlement susceptibility to assessing risks. To this aim, further consultation meetings and archival work must be conducted to attempt to retrieve the economic value of different infrastructure types and their rehabilitation costs. Additionally, our ability to integrate the societal factors conditioning infrastructure vulnerability (i.e., adaptive capacity, preparedness, monitoring capacity, emergency responses, regulatory frameworks, decision-making institutional organization, etc.) is still limited due to the difficulty to assess them, and to take into consideration both local and scientific perceptions. Pursuing multidisciplinary research remains essential to reconcile the social and physical components of risk, and develop more comprehensive and inclusive risk assessment frameworks.

In order to better understand the rapid deterioration of roads and to address maintenance challenges in Ilulissat, our attention was specifically directed towards existing infrastructure. Datasets principally dating from 2020 and 2021 were used to assess the susceptibility of the road network in response to current permafrost and climate conditions. Our framework opens up possibilities for integrating climate forecasts into estimate of future changes in TSSI and evaluation of permafrost thaw risks over unbuilt areas. Considering climate warming, permafrost thaw, landscape and hydrological changes in construction, maintenance, and planning practices is paramount for the cost-efficient management and development of Artic infrastructures.

6. Conclusions

This study presents a comprehensive susceptibility mapping framework for assessing permafrost thaw hazards, impacts, and infrastructure vulnerability. The current susceptibility of paved roads to permafrost thaw settlements (2012–2021) was documented for the settlement of Ilulissat, West-Greenland. Combining existing geotechnical data, infrastructure inventories, and recent research outcomes using remote sensing, a thaw settlement susceptibility index (TSSI) was computed for predefined road sections of 50 m in length.

39% of the paved roads assessed in Ilulissat were established on highly hazardous permafrost terrains. 33, 16, and 9% of these roads were very likely to suffer from thaw settlements, respectively due to the presence of frost-susceptible sediments, poor water drainage, or significant snow ploughing accumulations.

The impacts of thaw settlements on roads were evaluated based on the frequency of the repairs. During the study time frame, 3% of the roads had been repaved twice in less than three years and were thereby considered severely affected.

Additionally, 9% of the paved roads were classified as highly vulnerable to permafrost thaw due to their high level of damage and importance in ensuring access to critical facilities of the community.

Overall, the calculation of the TSSI showed that 12% of the paved roads in Ilulissat were significantly susceptible to permafrost thaw settlements and associated damages. The maps produced as part of the study are expected to support local infrastructure and risk management, and help optimize maintenance efforts and resources. Future research will focus on integrating climate projections into the mapping framework to predict the evolution of the TSSI for existing infrastructures, and the risk of permafrost thaw over unbuilt areas. Finally, more work remains needed to quantify the socioeconomic impacts of permafrost thaw-induced failures and factors conditioning infrastructure vulnerability.

Funding

This research was conducted as part of: the Nunataryuk project, funded by the European Union Horizon 2020 research and innovation programme under grant agreement No. 773421, and the Tarajulik project, funded by the Greenland Research Council under grant agreement no. 80.30.

CRediT authorship contribution statement

Johanna Scheer: Conceptualization, Formal analysis, Investigation, Methodology, Validation, Visualization, Writing – original draft, Writing – review & editing. **Soňa Tomaškovičová:** Conceptualization, Funding acquisition, Investigation, Project administration, Resources, Writing – review & editing. **Thomas Ingeman-Nielsen:** Conceptualization, Funding acquisition, Investigation, Project administration, Resources, Supervision, Writing – review & editing.

Declaration of competing interest

The authors declare that they have no known competing financial interests or personal relationships that could have appeared to influence the work reported in this paper.

Data availability

The geospatial layers integrated in this study were retrieved from the Technical Base Map by Asiaq Greenland Survey, available online at https://kortforsyning.asiaq.gl/, under the following terms of use https://kortforsyning.asiaq.gl/Downloads/EN_Termsofuse.pdf. The rasters and vectors produced as part of this study to evaluate the susceptibility of the road network to permafrost thaw settlements are openly available on Zenodo.

Acknowledgments

The authors thank Sarah Heller for contributing to the data acquisition in Ilulissat, and Christian Emil Johansen, Esben Fredskild Pedersen, and Rasmus Oskar Rossen, who helped with the digitization of the borehole logs. Additionally, the authors acknowledge Niels Mathias Rydbjerg for sharing data concerning snow removal. The authors are especially grateful to Asiaq Greenland Survey for providing access to their borehole archives and the Avannaata municipality for their valuable insights and feedback.

Appendix A. Local geospatial datasets

A.1. Characteristics

Table A.11
Technical characteristics of the datasets used as inputs in the susceptibility mapping framework.

Type	Dataset description	Origin	Date	Technical characteristics
Geotechnical information	1127 boreholes and shallow excavation logs	Asiaq Greenland Survey	1964-2006	Samples and stratigraphic layers characterized following the Danish Engineering Geological Practice (Larsen et al., 1995)
	98 boreholes and shallow excavation logs	Research (Technical University of Denmark) and commercial groups	2000-2021	
Remote-sensing information	Average thaw-season ground displacement	ESA Copernicus Sentinel-1	2015-2019	10 m pixel size raster
Infrastructure inventory	Pavement distresses (structural damages and surface deformations)	In-situ manual mapping by Scheer et al. (2023b)	2020-2021	Distress severity levels assessed following the standard ASTM D 6433–07 by ASTM International (2008)
	Cyclic repavement of the road network	In-situ manual mapping and local knowledge (Avannaata)	2012-2021	
	Land cover classification	Orthophotos and Map (TBM) by Asiaq Greenland Survey (2022)	2019-2022	Delineation of bedrock outcrops versus sedimentary basins
	Road network's geological substrate classification	Orthophotos and TBM by Asiaq Greenland Survey (2022)	2019-2022	Classified as bedrock, sediments or uncertain
	Water accumulation areas (naturally occurring or caused by disrupted drainage systems)	In-situ manual mapping by Scheer et al. (2023b), orthophotos and TBM by Asiaq Greenland Survey (2022)	2020-2022	
	Snow accumulation area caused by snow ploughing	Local knowledge (Avannaata) and in-situ manual mapping by Scheer et al. (2023b)	2017-2019	

A.2. Geotechnical data availability and distribution

The geotechnical data that were used to portray spatial variations in soil types are represented in Fig. A.11. A total of 1225 borehole and shallow excavation logs were digitized as part of the study, 955 of which could be classified based on the presence or absence of fine-grained sediments. The green dots on the figure correspond to the borehole locations where no fine-grained sediments were encountered within the first 3 m below ground surface. The red dots, representing 58% of all classified logs, indicate areas where the first 3 m of the stratigraphic profile contained fine-grained sediments. This map also classifies the study domain based on the availability of the geotechnical data. Dotted hexagonal cells inherited information from neighboring hexagons. Dashed hexagonal cells represent terrain units where information was unavailable.

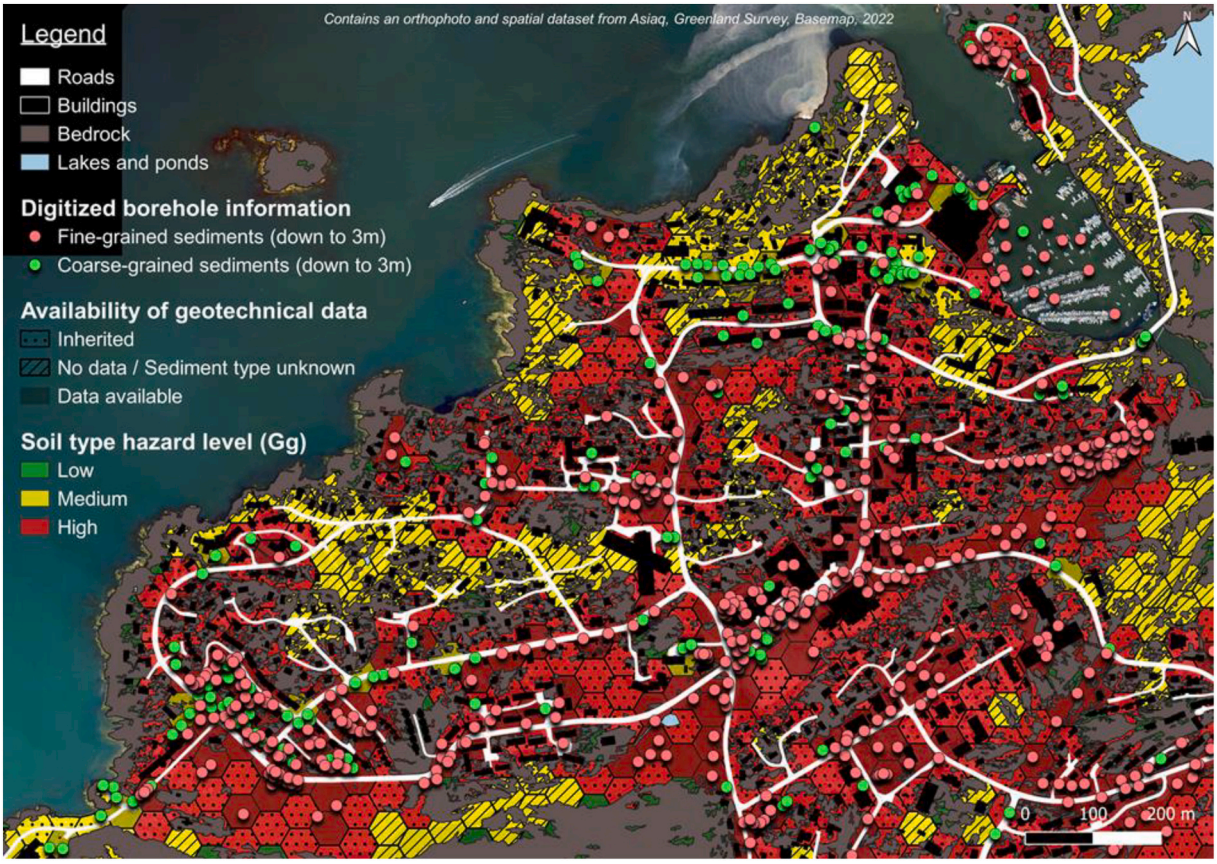

Fig. A.11. Borehole information used to assess the soil type hazard levels, G_g, across the study area. The green and red dots show the borehole classification based on the presence/absence of fine-grained sediments down to 3 m below the ground surface. The patterns overlaid onto the hexagonal terrain unit represent the availability of the geotechnical data. The map contains an orthophoto and spatial data from Asiaq, Greenland Survey, Basemap, 2022 (Asiaq Greenland Survey, 2022).

Appendix B. AHP weighted coefficients

B.1. Rating scale

The 9-point rating scale (Saaty, 1977) used for the pair-wise comparison of the hazard and vulnerability factors is presented as follows.

Table B.12
Saaty's pair-wise comparison 9-point rating scale.

Intensity of importance	Definition	Explanation
1	Equal importance	Two factors contribute equally to the objective
3	Somewhat more important	Experience and judgement slightly favour one over the other
5	Much more important	Experience and judgement strongly favour one over the other
7	Very much more important	Experience and judgement very strongly favour one over the other
9	Absolutely more important	The evidence favouring one over the other is of the highest possible validity
2, 4, 6, 8	Intermediate values	When compromise is needed

B.2. Hazard factor and class weights

The table hereunder summarizes the weighted coefficients obtained by AHP, representing the relative importance of each hazard factor and its respective classes in the likelihood of occurrence of thaw settlements, H.

Table B.13
AHP pair-wise comparison matrix, consistency ratios (CR), class and hazard factor weights used for the computation of the weighted hazard index.

Factors	***G***	***W***	***S***	**Factor weights (*w*)**
Substrate's frost susceptibility (*G*)	1			0.75
Water accumulation (*W*)	1/7	1		0.15
Snow accumulation (*S*)	1/6	1/2	1	0.10

(*continued on next page*)

Table B.13 (*continued*)

Factors	***G***	***W***	***S***	**Factor weights (*w*)**
CR: 0.07				
Class values	*Low*	*Medium*	*High*	**Class weights (*w*)**
Substrate's frost susceptibility (*G*)				
Low	1			0.07
Medium	3	1		0.1
High	9	6	1	0.76
CR:0.05				
Water accumulation (*W*)				
Low	1			0.08
Medium	3	1		0.19
High	8	5	1	0.74
CR: 0.04				
Snow accumulation (*S*)				
Low	1			0.07
Medium	6	1		0.35
High	7	2	1	0.58
CR: 0.03				

B.3. Vulnerability factor and class weights

The table hereunder summarizes the weighted coefficients obtained by AHP, representing the relative importance of each factor and its respective classes in the vulnerability of the roads, V.

Table B.14
AHP pair-wise comparison matrix, consistency ratios (CR), class and vulnerability factor weights used for the computation of the weighted vulnerability index.

Factors	***PCI***	***D***		**Factor weights (*w*)**
Level of damage (*PCI*)	1			0.67
Vulnerability to traffic disruptions (*D*)	1/2	1		0.33
CR: 0.00				
Class values	*Low*	*Medium*	*High*	**Class weights (*w*)**
Level of damage (*PCI*)				
Low	1			0.07
Medium	6	1		0.35
High	7	2	1	0.58
CR:0.03				
Vulnerability to traffic disruptions (*D*)				
Low	1			0.08
Medium	3	1		0.19
High	8	5	1	0.74
CR: 0.04				

Appendix C. Vulnerability factors

The maps presented hereinafter show the two factors contributing to the vulnerability of the roads, V. Fig. C.12a illustrates the pavement conditions of Ilulissat's road network, determined using the ASTM International (2008) standard. Fig. C.12b conveys the importance of each road section for the daily life and socioeconomic activities of the community. Roads symbolized in red provide access to critical facilities (red stars on the map) and have no alternative routes. They are, consequently, the most vulnerable to permafrost-induced hazards and traffic disruptions. The set of start and destination points used to analyze the road network and detect the presence of alternative routes is represented as small white dots and large red stars, respectively.

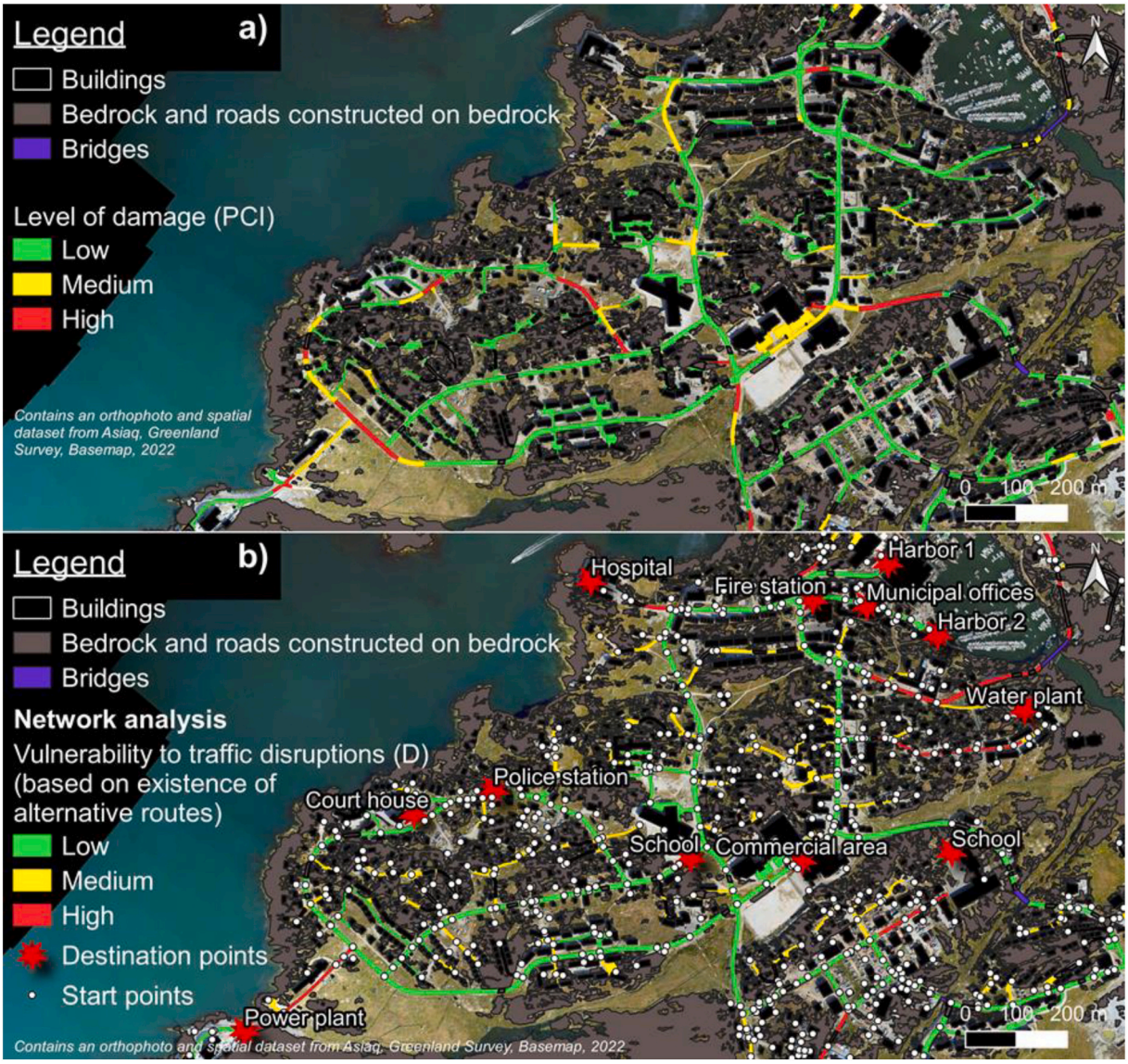

Fig. C.12. From top to bottom: (a) Road level of damage assessed with the Pavement Condition Index (*PCI*) (ASTM International, 2008), and (b) vulnerability to traffic disruptions (*D*). The maps contain an orthophoto and spatial data from Asiaq, Greenland Survey, Basemap, 2022 (Asiaq Greenland Survey, 2022).

References

Allard, M., Lemay, M., Barrette, C., L'Hérault, E., Sarrazin, D., Bell, T., Doré, G., 2012. 'Permafrost and climate change in nunavik and nunatsiavut: Importance for municipal and transportation infrastructures', Nunavik and Nunatsiavut: From science to policy. An Integrated Regional Impact Study (IRIS) of climate change and modernization, pp. 171–197.

Allard, M., L'Hérault, E., Aubé-Michaud, S., Carbonneau, A.-S., Mathon-Dufour, V., B.-St-Amour, A., Gauthier, S., 2023. Facing the challenge of permafrost thaw in nunavik communities: innovative integrated methodology, lessons learnt, and recommendations to stakeholders. Arctic Sci. 9 (3), 657–677.

AMAP Climate Change, 2019. 'An update to key findings of snow, water, ice and permafrost in the Arctic (SWIPA) 2017', Oslo, Norway. Arctic Monitoring and Assessment Programme (AMAP), p. 12.

Andersland, O.B., Ladanyi, B., 2003. Frozen Ground Engineering. John Wiley & Sons.

Asiaq Greenland Survey, 2022. Asiaq Map Supply Service. Data freely available online at: https://kortforsyning.asiaq.gl/ (last accessed on 11-05-2023), under the following terms of use https://kortforsyning.asiaq.gl/Downloads/EN_Termsofuse.pdf.

ASTM International, 2008. Standard Practice for Roads and Parking Lots Pavement Condition Index Surveys, Standard, West Conshohocken. PA 19428-2959,. United States.

Berdica, K., 2002. An introduction to road vulnerability: what has been done, is done and should be done. Transp. Policy 9 (2), 117–127.

Biskaborn, B.K., Smith, S.L., Noetzli, J., Matthes, H., Vieira, G., Streletskiy, D.A., Schoeneich, P., Romanovsky, V.E., Lewkowicz, A.G., Abramov, A., et al., 2019. Permafrost is warming at a global scale. Nat. Commun. 10 (1), 264.

Brooks, H., Doré, G., Locat, A., 2019. Quantitative risk analysis for linear infrastructure supported by permafrost: methodology and computer program. PhD thesis. Université Laval.

Brown, J., Ferrians Jr., O., Heginbottom, J., Melnikov, E., 1998. 'Revised february 2001. Circum-arctic map of permafrost and ground-ice conditions. Boulder, co: National snow and ice data center/world data center for glaciology, Digital media.

Canada, Engineers, 2016. PIEVC Engineering Protocol for Climate Change Infrastructure Vulnerability Assessment.

Cappelen, J., 2020. Weather observations from Greenland 1958-2019. Observation data with description. Technical Report 20-08, Danish Meteorological Institute. Available online at: https://www.dmi.dk/fileadmin/user_upload/Rapporter/TR/2020/DMIRep20-08.pdf, last accessed on 20-05-2023.

Chai, M., Mu, Y., Zhang, J., Ma, W., Liu, G., Chen, J., 2018. Characteristics of asphalt pavement damage in degrading permafrost regions: case study of the Qinghai–Tibet highway, china. J. Cold Reg. Eng. 32 (2), 05018003.

Daanen, R., Ingeman-Nielsen, T., Marchenko, S., Romanovsky, V., Foged, N., Stendel, M., Christensen, J., Hornbech Svensen, K., 2011. Permafrost degradation risk zone assessment using simulation models. Cryosphere Discuss. 5 (2), 1021–1053.

Dijkstra, E.W., 2022. A note on two problems in connexion with graphs. In: Edsger Wybe Dijkstra: His Life, Work, and Legacy, pp. 287–290.

Doré, G., Zubeck, H.K., 2009. Cold regions Pavement Engineering. Mcgraw-Hill Education.

Doré, G., Stephani, E., Lepage, J.M., 2022. An overview of major engineering challenges for developing transportation infrastructure in northern Canada. The School of Public Policy Publications 15 (1).
Duvillard, P.-A., Ravanel, L., Schoeneich, P., Deline, P., Marcer, M., Magnin, F., 2021. Qualitative risk assessment and strategies for infrastructure on permafrost in the French Alps. Cold Reg. Sci. Technol. 189, 103311.
Faber, M.H., 2008. Risk assessment in engineering: Principles, system representation & risk criteria, Technical report, ETH Zurich.
Guo, D., Wang, H., 2017. Permafrost degradation and associated ground settlement estimation under 2 c global warming. Clim. Dyn. 49, 2569–2583.
Haeberli, W., Whiteman, C., 2015. Snow and ice-related hazards, risks, and disasters: a general framework. In: Snow and Ice-Related Hazards, Risks, and Disasters. Elsevier, pp. 1–34.
Hagberg, A.A., Schult, D.A., Swart, P.J., 2008. Exploring network structure, dynamics, and function using Networkx. In: Varoquaux, G., Vaught, T., Millman, J. (Eds.), Proceedings of the 7th Python in Science Conference. Pasadena, CA USA, pp. 11–15.
Hjort, J., Karjalainen, O., Aalto, J., Westermann, S., Romanovsky, V.E., Nelson, F.E., Etzelmüller, B., Luoto, M., 2018. Degrading permafrost puts arctic infrastructure at risk by mid-century. Nat. Commun. 9 (1), 1–9.
Hjort, J., Streletskiy, D., Doré, G., Wu, Q., Bjella, K., Luoto, M., 2022. Impacts of permafrost degradation on infrastructure. Nat. Rev. Earth Environ. 3 (1), 24–38.
Hong, E., Perkins, R., Trainor, S., 2014. Thaw settlement hazard of permafrost related to climate warming in Alaska. Arctic 93–103.
Ingeman-Nielsen, T., Lemay, M., Allard, M., Barrette, C., Bjella, K., Brooks, H., Carbonneau, A.-S., Doré, G., Foged, N., Lading, T., et al., 2018. Built infrastructure, in 'Adaptation Actions for a Changing Arctic: Perspectives from the Baffin Bay/Davis Strait Region', Arctic Monitoring and Assessment Programme (AMAP), pp. 261–306.
Jenks, G.F., 1967. The data model concept in statistical mapping. In: International yearbook of cartography, 7, pp. 186–190.
Jungsberg, L., Herslund, L.B., Nilsson, K., Wang, S., Tomaškovičová, S., Madsen, K., Scheer, J., Ingeman-Nielsen, T., 2022. Adaptive capacity to manage permafrost degradation in northwest Greenland. Polar Geogr. 45 (1), 58–76.
Larsen, G., Frederiksen, J., Villumsen, A., Fredericia, J., Gravesen, P., Foged, N., Knudsen, B., Baumann, J., 1995. A guide to engineering geological soil description. Technical Report 1, Danish Geotechnical Society. dgf-Bulletin 1.
Larsen, J.N., Schweitzer, P., Abass, K., Doloisio, N., Gartler, S., Ingeman-Nielsen, T., Ingimundarson, J.H., Jungsberg, L., Meyer, A., Rautio, A., et al., 2021. Thawing permafrost in arctic coastal communities: a framework for studying risks from climate change. Sustainability 13 (5), 2651.
Lavell, A., Oppenheimer, M., Diop, C., Hess, J., Lempert, R., Li, J., Muir-Wood, R., Myeong, S., Moser, S., Takeuchi, K., et al., 2012. Climate change: new dimensions in disaster risk, exposure, vulnerability, and resilience. In: Managing the risks of extreme events and disasters to advance climate change adaptation: Special report of the intergovernmental panel on climate change. Cambridge University Press, pp. 25–64.
Li, R., Zhang, M., Konstantinov, P., Pei, W., Tregubov, O., Li, G., 2022. Permafrost degradation induced thaw settlement susceptibility research and potential risk analysis in the Qinghai-Tibet plateau. Catena 214, 106239.
Liu, Z., Zhu, Y., Chen, J., Cui, F., Zhu, W., Liu, J., Yu, H., 2023. Risk zoning of permafrost thaw settlement in the Qinghai–Tibet engineering corridor. Remote Sens. 15 (15), 3913.
Monroe, A., 2017. Pavementconditionindex. https://github.com/brandnewbox/pavement_condition_index.git.
Nelson, F.E., Anisimov, O.A., Shiklomanov, N.I., 2002. Climate change and hazard zonation in the circum-arctic permafrost regions. Nat. Hazards 26, 203–225.
Ni, J., Wu, T., Zhu, X., Wu, X., Pang, Q., Zou, D., Chen, J., Li, R., Hu, G., Du, Y., et al., 2021. Risk assessment of potential thaw settlement hazard in the permafrost regions of Qinghai-Tibet plateau. Sci. Total Environ. 776, 145855.
Obu, J., Westermann, S., Bartsch, A., Berdnikov, N., Christiansen, H.H., Dashtseren, A., Delaloye, R., Elberling, B., Etzelmüller, B., Kholodov, A., et al., 2019. Northern hemisphere permafrost map based on TTOP modelling for 2000–2016 at 1 km2 scale. Earth Sci. Rev. 193, 299–316.
Ramage, J., Jungsberg, L., Meyer, A., Gartler, S., 2022. no longer solid: perceived impacts of permafrost thaw in three arctic communities. Polar Geogr. 45 (3), 226–239.
Rantanen, M., Karpechko, A.Y., Lipponen, A., Nordling, K., Hyvärinen, O., Ruosteenoja, K., Vihma, T., Laaksonen, A., 2022. The arctic has warmed nearly four times faster than the globe since 1979. Commun. Earth Environ. 3 (1), 168.
Rasch, M., 2000. Holocene relative sea level changes in Disko Bugt, west Greenland. J. Coast. Res. 306–315.
Rudy, A., Morse, P., Kokelj, S., Sladen, W., Smith, S., 2019. A new protocol to map permafrost geomorphic features and advance thaw-susceptibility modelling. In: Cold Regions Engineering 2019. American Society of Civil Engineers Reston, VA, pp. 661–669.
Saaty, T.L., 1977. A scaling method for priorities in hierarchical structures. J. Math. Psychol. 15 (3), 234–281.
Saaty, T.L., 2008. Decision making with the analytic hierarchy process. Int. J. Services Sci. 1 (1), 83–98.
Scheer, J., Ingeman-Nielsen, T., 2023. Classification of frozen cores from Ilulissat, Greenland: Boreholes drilled in 2018 and 2021, Technical report. DTU Sustain.
Scheer, J., Caduff, R., How, P., Marcer, M., Strozzi, T., Bartsch, A., Ingeman-Nielsen, T., 2023a. Thaw- season InSAR surface displacements and frost susceptibility mapping to support community-scale planning in Ilulissat, West Greenland. Remote Sens. 15 (13), 3310.
Scheer, J., Ingeman-Nielsen, T., Tomaškovičová, S., 2023b. Geospatial Analysis of Road Conditions and Hazardous Factors in Communities on Continuous vs. Sporadic Permafrost in Greenland. Available at SSRN. https://doi.org/10.2139/ssrn.4544058 (Under review).
Seto, J., Arenson, L., Cousineau, G., 2012. Vulnerability to climate change assessment for a highway constructed on permafrost. In: Cold Regions Engineering 2012: Sustainable Infrastructure Development in a Changing Cold Environment, pp. 515–524.
Shahabi, H., Hashim, M., 2015. Landslide susceptibility mapping using GIS-based statistical models and remote sensing data in tropical environment. Sci. Rep. 5 (1), 9899.
Statistics Greenland, 2017. Statistisk Årbog 2017. Available online at: https://stat.gl/sa/saD2017.pdf. last accessed on 20-05-2023.
Streletskiy, D.A., Suter, L.J., Shiklomanov, N.I., Porfiriev, B.N., Eliseev, D.O., 2019. Assessment of climate change impacts on buildings, structures and infrastructure in the Russian regions on permafrost. Environ. Res. Lett. 14 (2), 025003.
Tomaškovičová, S., Ingeman-Nielsen, T., 2023. Quantification of freeze–thaw hysteresis of unfrozen water content and electrical resistivity from time lapse measurements in the active layer and permafrost. Permafr. Periglac. Process. 1–19.
Yalcin, A., 2008. GIS-based landslide susceptibility mapping using analytical hierarchy process and bivariate statistics in ardesen (turkey): comparisons of results and confirmations. Catena 72 (1), 1–12.